

## Supporting Information

# A Localized Enantioselective Catalytic Site on Short DNA Sequences and their Amphiphiles

Jun Guo,<sup>a, ‡</sup> Danyu Wang,<sup>a, b, ‡</sup> Evangelia Pantatosaki,<sup>c</sup> Huihui Kuang,<sup>a</sup> George K. Papadopoulos,<sup>c, d</sup> Michael Tsapatsis<sup>a, b, e, \*</sup> and Efrosini Kokkoli<sup>a, b, \*</sup>

- 
- a Institute for NanoBiotechnology, Johns Hopkins University, Baltimore, Maryland 21218, United States  
b Department of Chemical and Biomolecular Engineering, Johns Hopkins University, Baltimore, MD 21218, United States  
c School of Chemical Engineering, National Technical University of Athens, 15780 Athens, Greece  
d Institute for Medical Engineering and Science, Massachusetts Institute of Technology, Cambridge, MA 02139, United States  
e Applied Physics Laboratory, Johns Hopkins University, Laurel, MD 20723, United States  
‡ These authors contributed equally to this work.  
\* Corresponding authors:  
Michael Tsapatsis: [tsapatsis@jhu.edu](mailto:tsapatsis@jhu.edu)  
Efrosini Kokkoli: [kokkoli@jhu.edu](mailto:kokkoli@jhu.edu)

### Table of Contents

Experimental Procedures .....	2
References .....	6
Supplementary Schemes .....	8
Supplementary Tables .....	10
Supplementary Figures .....	16
<sup>1</sup> H-NMR Spectra and <sup>13</sup> C-NMR Spectra.....	38
HPLC Chromatogram .....	44
Calculation of Conversion of (1a).....	45

## Experimental Procedures

### Materials

ssDNA was purchased from Integrated DNA Technologies (Coralville, IA) and the strand concentrations were determined by measuring the absorbance at 260 nm using the extinction coefficient values provided by Integrated DNA Technologies. All other chemicals and materials were purchased from Sigma-Aldrich (St Louis, MO) and used without further purification unless stated otherwise. The organic compounds (1a and 3a) employed for catalysis and calibration were synthesized based on literature reports (see p. 38 for  $^1\text{H}$  NMR and  $^{13}\text{C}$  NMR).<sup>1-2</sup> Cu(II) complexes (dmbipy-Cu) were prepared as reported previously and characterized by MALDI-TOF MS (Table S2).<sup>3</sup>

### Methods

$^1\text{H}$  NMR and  $^{13}\text{C}$  NMR spectra were recorded on a Bruker Advance 400 MHz FT-NMR spectrometers with  $\text{CDCl}_3$  at room temperature. Proton chemical shifts are referenced to TMS (0.00 ppm, in  $\text{CDCl}_3$ ) and  $^{13}\text{C}$  chemical shifts are referenced to TMS (77.16 ppm, in  $\text{CDCl}_3$ ). ssDNA-amphiphiles were purified by an Agilent 1260 Infinity II high performance liquid chromatography (HPLC) and characterized by MALDI-TOF MS. Analysis of DNA catalytic reactions was performed on an Agilent 1260 Infinity II HPLC with the eluents of hexane and isopropanol (*i*-PrOH), using a Daicel Chiralcel OD-H column (250  $\times$  4.6 mm) at 25  $^\circ\text{C}$ . In all experiments, MilliQ water (Millipore Inc.) with a typical resistivity of 18.2  $\text{m}\Omega/\text{cm}$  was used. All catalysis reactions were carried out in 20 mM MOPS buffer (pH 6.5) unless otherwise stated. Circular dichroism (CD) studies were carried out at 4  $^\circ\text{C}$  on an Aviv 420 spectropolarimeter in a 0.1 cm quartz cuvette, with DNA concentrations at 50  $\mu\text{M}$  for samples in water (or 15  $\mu\text{M}$  for samples in methanol-water mixtures ( $v/v = 50/50$ )) and the spectra were collected from 320-200 nm with a 1 nm step size, averaging for 3 s at each step. The background CD spectrum of corresponding buffer solution was subtracted from every CD curve. Melting temperature measurements were carried out on an Aviv 14DS UV-Vis spectrophotometer with Neslab RET-111 temperature controller in a 1 cm quartz cuvette with a 1  $^\circ\text{C}$  temperature step.

### Synthesis of N-hydroxysuccinimide activated hydrophobic tail

The dendron tail, methyl 3,4-bis[*p*-(*n*-dodecan-1-yloxy)benzyloxy]benzoate, was synthesized (see p. 42 for  $^1\text{H}$  NMR and  $^{13}\text{C}$  NMR) and was hydrolyzed to 3,4-bis[*p*-(*n*-dodecan-1-yloxy)benzyloxy]benzoic acid following a reported protocol.<sup>4</sup> The carboxylic acid group on 3,4-bis[*p*-(*n*-dodecan-1-yloxy)benzyloxy]benzoic acid was activated by *N*-hydroxysuccinimide (NHS), using the following protocol: diisopropylcarbodiimide (1.26 g, 10 mmol) dissolved in 5 mL dichloromethane were added dropwise at 0  $^\circ\text{C}$  under argon atmosphere to a mixture of 3,4-bis[*p*-(*n*-dodecan-1-yloxy)benzyloxy]benzoic acid (3.52 g, 5 mmol), NHS (1.15 g, 10 mmol) and dimethylaminopyridine (9.2 mg, 0.075 mmol) in 25 mL dichloromethane. The mixture was stirred at 0  $^\circ\text{C}$  for 2 h and then at 20  $^\circ\text{C}$  for 24 h. Diisopropylurea was then removed as an insoluble side product by filtration. The solvent was then removed using dynamic vacuum. The crude product was purified by column chromatography on silica gel (eluant: ethyl acetate-hexane mixture ( $v/v=1:3$ );  $R_f = 0.7$ ) to obtain the pure NHS-activated 3,4-bis[*p*-(*n*-dodecan-1-yloxy)benzyloxy]benzoic acid as a white solid (3 g, 75% yield).

### Synthesis of ssDNA-amphiphiles

The ssDNA-amphiphiles were synthesized based on a previously published protocol<sup>5</sup> that was modified slightly (Scheme S3). 1.5x molar excess (based on the molar number of phosphates on the ssDNA backbone) of cetyl trimethylammonium bromide (CTAB) was added to an aqueous solution of an amino-modified ssDNA sequence, leading to the formation of a CTAB-ssDNA precipitate. The CTAB-ssDNA precipitate was collected by centrifuge and dried under dynamic vacuum. The CTAB-ssDNA precipitate was then dissolved in a mixture of *N,N*-dimethylformamide (DMF) and dimethyl sulfoxide (DMSO) ( $v/v=9:1$ ) at 65  $^\circ\text{C}$  (100 nmol CTAB-ssDNA precipitate per 300  $\mu\text{L}$  solvent). 10x molar excess (based on moles of the entire DNA sequence) of *N*-hydroxysuccinimide (NHS) functionalized hydrophobic tail was added to the solution and allowed to react under stirring for 24 h at 65  $^\circ\text{C}$ . The DMF-DMSO mixture was then evaporated under dynamic vacuum. Lithium perchlorate (2.5% w/v in acetone) was added next to dissolve the unreacted tails and CTAB. The ssDNA-amphiphile and the unreacted ssDNA were collected by centrifuge and dissolved in water. The ssDNA-amphiphile was separated from the unreacted ssDNA by reverse phase high performance liquid chromatography (RP-HPLC) on an Agilent Zorbax 300SB-C3 column, using a gradient from 95% buffer A to 98% buffer B over 20 min at 1 mL/min (Buffer A: water with 100 mM HFIP and 14.4 mM TEA; buffer B: methanol with 100 mM HFIP and 14.4 mM TEA). The synthesized ssDNA-amphiphiles were characterized by matrix assisted laser desorption ionization-time of flight (MALDI-TOF) mass spectrometry (MS) (Table S3).

### Preparation of CD samples in water

An aqueous solution of a ssDNA sequence (15  $\mu\text{L}$ , 1 mM) and its complementary ssDNA sequence (15  $\mu\text{L}$ , 1 mM) were added to MOPS buffer (270  $\mu\text{L}$ , final concentration: 20 mM, pH 6.5) to prepare 300  $\mu\text{L}$  aqueous solution with 50  $\mu\text{M}$  final DNA concentration. Measurements for the HT21 sequence were also performed in MOPS buffer with 0.1 M NaCl. For all samples, the tube was heated in the dry-bath heater to 95  $^\circ\text{C}$ , kept for 3 min, and the heater was turned off to let the tube slowly cool

down to room temperature. For measurements with dmbipy-Cu, a solution of dmbipy-Cu (1.5  $\mu\text{L}$ , 10 mM) was added to the sample.

### Preparation of CD samples in methanol-water

An aqueous solution of a ssDNA sequence (4.5  $\mu\text{L}$ , 1 mM) and its complementary ssDNA sequence (4.5  $\mu\text{L}$ , 1 mM) were added to MOPS buffer (141  $\mu\text{L}$ , final concentration: 20 mM, pH 6.5). The tube was heated in the dry-bath heater to 95  $^{\circ}\text{C}$ , kept for 3 min, and the heater was turned off to let the tube slowly cool down to room temperature. For measurements with dmbipy-Cu, a solution of dmbipy-Cu (0.45  $\mu\text{L}$ , 10 mM) was added to the sample. 150  $\mu\text{L}$  methanol was then added to prepare the methanol-water mixture (v/v = 50/50) with 15  $\mu\text{M}$  final DNA concentration.

### Diels-Alder reaction in water

An aqueous solution of a ssDNA sequence (50  $\mu\text{L}$ , 1 mM) and its complementary ssDNA sequence (50  $\mu\text{L}$ , 1 mM) were added to MOPS buffer (840  $\mu\text{L}$ , final concentration: 20 mM, pH 6.5). The tube was heated in a dry-bath heater to 95  $^{\circ}\text{C}$ , kept for 3 min, and the heater was then turned off to let the tube slowly cool down to room temperature. A solution of dmbipy-Cu (50  $\mu\text{L}$ , 1 mM) was added and the solution was stirred for 0.5 h at 4  $^{\circ}\text{C}$ . Then, aza-chalcone (**1a**) in  $\text{CH}_3\text{CN}$  (10  $\mu\text{L}$  of 0.1 M solution) was added. The reaction was initiated by the addition of freshly distilled cyclopentadiene (**2**) (5.6  $\mu\text{L}$ , 67 eq.) and the mixture was stirred for 3 h at 4  $^{\circ}\text{C}$ , followed by extraction with diethyl ether (3 times, 3 mL diethyl ether per time) and filtration through a short pad of silica gel. The solvent was removed under reduced pressure. The conversion, diastereoselectivity (*endo:exo*) and enantiomeric excess (ee) were determined by chiral HPLC (see p. 44 for a representative HPLC chromatogram and p. 45 for calculation of (**1a**) conversion).

HPLC condition: Product **3a**: Daicel chiralcel OD-H, hexane/*i*-PrOH 98:2, 0.5 mL/min, 212 nm. Retention times: 11.5 (*Si-exo*), 12.8 min (*Re-exo*); 14.5 (*Re-endo*), 18.5 min (*Si-endo*).<sup>6</sup>

### Diels-Alder reaction in methanol-water

An aqueous solution of a ssDNA sequence (15  $\mu\text{L}$ , 1 mM) and its complementary ssDNA sequence (15  $\mu\text{L}$ , 1 mM) were added to MOPS buffer (445  $\mu\text{L}$ , final concentration: 20 mM, pH 6.5). The tube was heated in a dry-bath heater to 95  $^{\circ}\text{C}$ , kept for 3 min, and the heater was then turned off to let the tube slowly cool down to room temperature. A solution of dmbipy-Cu (15  $\mu\text{L}$ , 1 mM) was added and the solution was stirred for 0.5 h at 4  $^{\circ}\text{C}$ . Then, 500  $\mu\text{L}$  methanol and aza-chalcone (**1a**) in  $\text{CH}_3\text{CN}$  (10  $\mu\text{L}$  of 0.1 M solution) were added. The reaction was initiated by the addition of freshly distilled cyclopentadiene (**2**) (5.6  $\mu\text{L}$ , 67 eq.) and the mixture was stirred for 48 h at 4  $^{\circ}\text{C}$ , followed by extraction with diethyl ether (3 times, 3 mL diethyl ether per time) and filtration through a short pad of silica gel. The solvent was removed under reduced pressure. The conversion, diastereoselectivity (*endo:exo*) and ee were determined by chiral HPLC.

HPLC condition: Product **3a**: Daicel chiralcel OD-H, hexane/*i*-PrOH 98:2, 0.5 mL/min, 212 nm. Retention times: 11.5 (*Si-exo*), 12.8 min (*Re-exo*); 14.5 (*Re-endo*), 18.5 min (*Si-endo*).<sup>6</sup>

### Friedel-Crafts alkylation in water

An aqueous solution of a ssDNA sequence (50  $\mu\text{L}$ , 1 mM) and its complementary ssDNA sequence (50  $\mu\text{L}$ , 1 mM) were added to MOPS buffer (840  $\mu\text{L}$ , final concentration: 20 mM, pH 6.5). The tube was heated in a dry-bath heater to 95  $^{\circ}\text{C}$ , kept for 3 min, and the heater was then turned off to let the tube slowly cool down to room temperature. A solution of dmbipy-Cu (50  $\mu\text{L}$ , 1 mM) was added and the solution was stirred for 0.5 h at 4  $^{\circ}\text{C}$ . Then,  $\alpha,\beta$ -unsaturated 2-acyl imidazole (**1b**) in  $\text{CH}_3\text{CN}$  (10  $\mu\text{L}$  of 0.1 M solution) was added. The reaction was initiated by the addition of pyrrole in  $\text{CH}_3\text{CN}$  (10  $\mu\text{L}$  of 0.5 M solution, 5 eq.) and the mixture was stirred for 7 days at 4  $^{\circ}\text{C}$ , followed by extraction with diethyl ether (3 times, 3 mL diethyl ether per time) and filtration through a short pad of silica gel. The solvent was removed under reduced pressure. The conversion and ee were determined by chiral HPLC.

HPLC condition: Product **4b**: Daicel chiralcel OD-H, heptane/*i*-PrOH 90:10, 0.5 mL/min, 254 nm. Retention times: 26.2 (S enantiomer), 27.5 min (R enantiomer).

### Michael addition in water

An aqueous solution of a ssDNA sequence (50  $\mu\text{L}$ , 1 mM) and its complementary ssDNA sequence (50  $\mu\text{L}$ , 1 mM) were added to MOPS buffer (840  $\mu\text{L}$ , final concentration: 20 mM, pH 6.5). The tube was heated in a dry-bath heater to 95  $^{\circ}\text{C}$ , kept for 3 min, and the heater was then turned off to let the tube slowly cool down to room temperature. A solution of dmbipy-Cu (50  $\mu\text{L}$ , 1 mM) was added and the solution was stirred for 0.5 h at 4  $^{\circ}\text{C}$ . Then,  $\alpha,\beta$ -unsaturated 2-acyl imidazole (**1b**) in  $\text{CH}_3\text{CN}$  (10  $\mu\text{L}$  of 0.1 M solution) was added. The reaction was initiated by the addition of dimethyl malonate (11.4  $\mu\text{L}$ , 100 eq.) and the mixture was stirred for 7 days at 4  $^{\circ}\text{C}$ , followed by extraction with diethyl ether (3 times, 3 mL diethyl ether per time) and filtration through a short pad of silica gel. The solvent was removed under reduced pressure. The conversion and ee were determined by chiral HPLC.

HPLC condition: Product **5b**: Daicel chiralcel OD-H, heptane/*i*-PrOH 90:10, 0.5 mL/min, 254 nm. Retention times: 55.6 (S enantiomer), 44.5 min (R enantiomer).

## Melting temperature measurements

The melting temperatures were measured on an Aviv 14DS UV-Vis spectrophotometer with Neslab RET-111 temperature controller in a 1 cm quartz cuvette. Concentrations of DNA samples are given in the figure captions and Table S6. The absorbance was measured at 268 nm every 1 °C in phosphate buffer (100 mM, pH 6.5). The samples were held at 80 °C for 10 min and then cooled from 80 °C to 1 °C and heated from 1 °C to 80 °C at 0.2 °C/min. No hysteresis was seen using this temperature gradient. For st-DNA the sample was held at 1 °C for 10 min and then heated to 95 °C at 0.2 °C/min. For the “8-4, 5” and “8-4, 5-amph.”, absorbance was also measured at 268 nm every 1 °C in a 50/50 (v/v) mixture of methanol and phosphate buffer (100 mM, pH 6.5). The samples were held at 50 °C for 10 min and then cooled from 50 °C to 1 °C and heated from 1 °C to 50 °C at 0.2 °C/min. No hysteresis was seen using this temperature gradient. The melting temperatures for all samples were determined from three independent measurements using the first derivative method as described elsewhere.<sup>7</sup>

## Binding constant measurements

The binding constants of dmbipy-Cu to different DNA sequences were determined by UV/Vis titration as discussed elsewhere.<sup>3</sup> All measurements were performed in MOPS buffer (20 mM, pH 6.5) at 4 °C. The concentration of dmbipy-Cu was 50 μM and the concentration of the DNA sequences (in base pairs) during the titration process ranged from 32 μM to 160 μM. The absorbance was measured at 307 nm.

## Modeling details

Two dsDNA molecules with 21 base pairs of “21” and “21-10, 11” sequences, were modeled in atomistic detail,<sup>8</sup> the sequence of bases along the two strands of the modeled DNAs are shown in Table S4.

For the modeling of the Cu(II) complex of 4,4'-dimethyl-2,2'-bipyridine (dmbipy-Cu), the crystallographic information file (CIF)<sup>9</sup> of the solid state structure was used. The coordinated nitrate groups were removed, following vibrational spectroscopy experiments<sup>9</sup> which report that the structure of the solid state dmbipy-Cu complex does not change significantly upon solvation in water, except for the displacement of the nitrate groups by water molecules due to nitrate's low association constant to copper.

Molecular Dynamics (MD) simulations were conducted in the isobaric, isothermal ensemble ( $P = 1$  bar,  $T = 310$  K); the numerical integration of the differential equations of motion<sup>10-12</sup> was performed by means of the AMBER94<sup>13</sup> force field. In the absence of non-bonded parameters for the copper(II) atom in bio-inorganic compounds, the Lennard-Jones parameters for the copper(II) atom were taken from Babu et al.,<sup>14</sup> wherein is reported that the parameters are compatible with the AMBER force field and reproduce (i) the number and structure of the first-shell coordination waters around Cu(II), capturing accurately its octahedral coordination geometry, namely the four square-planar equatorial and two axial positions for coordinating ligands; (ii) its relative hydration free energy; and (iii) the average Cu(II)-O (water) distance. In addition, the adopted Lennard-Jones parameters have been successfully used in simulation studies of copper(II)-based organic compounds known as Casiopeínas@ intercalating the DNA.<sup>15-16</sup> The partial charges on the dmbipy-Cu atoms were derived using the R.E.D. server<sup>17</sup> by employing the Restrained Electrostatic Potential methodology<sup>18-19</sup> to reproduce the molecular electrostatic potential computed via density functional theory calculations, using the B3LYP exchange correlation functional with basis set 6-31G (d) level of theory. The equilibrium values for the Cu-N bond length, and Cu-N-C and N-Cu-N angles, were set equal to the crystallographic values<sup>9</sup>. To validate the choice of parameters, the dmbipy-Cu structural observables appearing in Table S5 were computed and compared with available crystallographic data; the computed and experimental values are in good agreement, indicating that the model accurately captures the dmbipy-Cu geometry.

The rhombic dodecahedron simulation box dimensions were set so that to ensure at least 3 nm thickness for the solvent surrounding the dmbipy-Cu and DNA molecules in all directions. This value is well above the minimum value of 0.8 to 1.2 nm recommended in protocols for nucleic acids simulations.<sup>20</sup> Randomly selected water molecules were replaced by the appropriate number of Na cations to neutralize the system. The TIP3P water model was employed,<sup>21</sup> which enables high computational efficiency and has been successfully combined with the AMBER force fields in modeling nucleic acids hydration.<sup>22</sup>

For the equilibration of the system, prior to the MD production runs, we followed the equilibration protocol described in our previous work on the binding dynamics of siRNA with lipopeptide molecules.<sup>23</sup> The Berendsen algorithm was utilized so that to allow for fluctuating the pressure tensor (diagonal components) isotropically under the constrain of a constant trace (the pressure),<sup>24</sup> with a time constant of 2.0 ps; the isothermal compressibility of water was set equal to  $4.5 \times 10^{-5}$  bar<sup>-1</sup>. For the thermostating a velocity-rescaling scheme<sup>25</sup> was employed on two separate groups, namely the DNA with the dmbipy-Cu, and the ionic solvent, with a time constant of 0.1 ps. For the dispersion interactions a shifted cutoff of 1 nm was applied. Bond lengths were constrained as usually in most biomolecular systems.<sup>26-27</sup> The smooth particle-mesh Ewald method<sup>28</sup> was employed for the computation of the electrostatic interactions. MD trajectories were produced up to 230 ns, using a timestep of 2 fs, and recorded every 10 ps. The geometrical characteristics of the dsDNAs were extracted using CURVES+.<sup>29</sup> Visualization of the MD trajectory and image rendering was performed ultimately by means of VMD.<sup>30</sup>

In the post-processing stage, the distance between the minor groove base atoms and the copper atom was computed as the minimum distance of all the following minor groove base atoms with the copper atom. For “21” sequence, the minor groove base atoms include N3 of adenine, C2 of adenine and O2 of thymine. For “21-10, 11” sequence, the minor groove base atoms include N3 of adenine, C2 of adenine, O2 of thymine, N3 of guanine, N2 of guanine and O2 of cytosine. The notation of the base atoms follows the standard IUPAC-IUB numbering convention for the nucleic acid bases.<sup>31</sup> The computed distances were binned to bins of 0.1 nm width, and, subsequently, normalized histograms over the total number of configurations (time frames) were constructed.

The same procedure was followed for computing the distance between the minor groove base atoms and each of the pyridine methyl carbons. Also, the same procedure was followed for computing the distance between the minor or major groove base atoms and the dmbipy-Cu for all the atoms of the dmbipy-Cu. For “21” sequence, the major groove base atoms include N7 of adenine, N6 of adenine and O4 of thymine; for “21-10, 11” sequence, the major groove base atoms include N7 of adenine, N6 of adenine, O4 of thymine, N7 of guanine, O6 of guanine and N4 of cytosine.

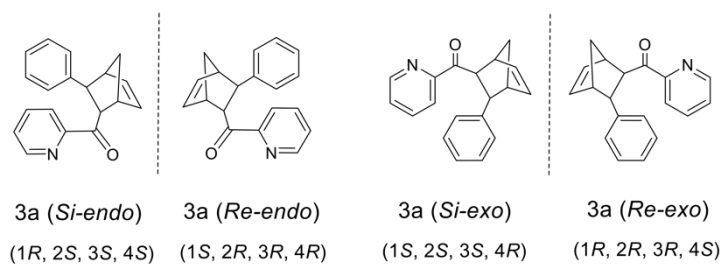
In Figures S19 and S23, computations for the base pairs at the edges of the DNA were excluded due to spurious values caused by terminal base-pair fraying events, a known artifact in nucleic acids simulations using the AMBER force fields.<sup>32</sup>

## References

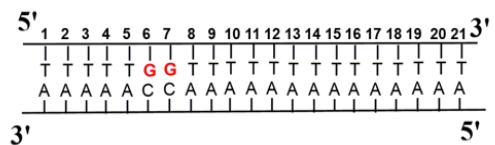
- (1) Otto, S.; Bertoncin, F.; Engberts, J. B., Lewis acid catalysis of a Diels–Alder reaction in water. *J. Am. Chem. Soc.* **1996**, *118* (33), 7702-7707.
- (2) Evans, D. A.; Fandrick, K. R.; Song, H.-J., Enantioselective Friedel–Crafts alkylations of  $\alpha$ ,  $\beta$ -unsaturated 2-acyl imidazoles catalyzed by bis (oxazoliny) pyridine–scandium (III) triflate complexes. *J. Am. Chem. Soc.* **2005**, *127* (25), 8942-8943.
- (3) Roelfes, G.; Boersma, A. J.; Feringa, B. L., Highly enantioselective DNA-based catalysis. *Chem. Commun.* **2006**, (6), 635-637.
- (4) Percec, V.; Cho, W.-D.; Ungar, G.; Yeardley, D. J., Synthesis and structural analysis of two constitutional isomeric libraries of AB<sub>2</sub>-based monodendrons and supramolecular dendrimers. *J. Am. Chem. Soc.* **2001**, *123* (7), 1302-1315.
- (5) Kuang, H.; Gartner, T. E.; de Mello, M. D.; Guo, J.; Zuo, X.; Tsapatsis, M.; Jayaraman, A.; Kokkoli, E., ssDNA-amphiphile architecture used to control dimensions of DNA nanotubes. *Nanoscale* **2019**, *11* (42), 19850-19861.
- (6) Wang, C.; Qi, Q.; Li, W.; Dang, J.; Hao, M.; Lv, S.; Dong, X.; Gu, Y.; Wu, P.; Zhang, W., A Cu (II)–ATP complex efficiently catalyses enantioselective Diels–Alder reactions. *Nat. Commun.* **2020**, *11* (1), 1-8.
- (7) Akhter, M. Z.; Sharma, A.; Rajeswari, M. R., Interaction of adriamycin with a promoter region of hmga1 and its inhibitory effect on HMGA1 expression in A431 human squamous carcinoma cell line. *Mol. Biosyst.* **2011**, *7* (4), 1336-1346.
- (8) Li, S.; Olson, W. K.; Lu, X.-J., Web 3DNA 2.0 for the analysis, visualization, and modeling of 3D nucleic acid structures. *Nucleic Acids Res.* **2019**, *47* (W1), W26-W34.
- (9) Draksharapu, A.; Boersma, A. J.; Leising, M.; Meetsma, A.; Browne, W. R.; Roelfes, G., Binding of copper (II) polypyridyl complexes to DNA and consequences for DNA-based asymmetric catalysis. *Dalton Trans.* **2015**, *44* (8), 3647-3655.
- (10) Abraham, M. J.; Murtola, T.; Schulz, R.; Páll, S.; Smith, J. C.; Hess, B.; Lindahl, E., GROMACS: High performance molecular simulations through multi-level parallelism from laptops to supercomputers. *SoftwareX* **2015**, *1*, 19-25.
- (11) Van Der Spoel, D.; Lindahl, E.; Hess, B.; Groenhof, G.; Mark, A. E.; Berendsen, H. J., GROMACS: fast, flexible, and free. *J. Comput. Chem.* **2005**, *26* (16), 1701-1718.
- (12) Berendsen, H. J.; van der Spoel, D.; van Drunen, R., GROMACS: a message-passing parallel molecular dynamics implementation. *Comput. Phys. Commun.* **1995**, *91* (1-3), 43-56.
- (13) Cornell, W. D.; Cieplak, P.; Bayly, C. I.; Gould, I. R.; Merz, K. M.; Ferguson, D. M.; Spellmeyer, D. C.; Fox, T.; Caldwell, J. W.; Kollman, P. A., A second generation force field for the simulation of proteins, nucleic acids, and organic molecules. *J. Am. Chem. Soc.* **1995**, *117* (19), 5179-5197.
- (14) Babu, C. S.; Lim, C., Empirical force fields for biologically active divalent metal cations in water. *The Journal of Physical Chemistry A* **2006**, *110* (2), 691-699.
- (15) Galindo-Murillo, R.; Ruiz-Azuara, L.; Moreno-Esparza, R.; Cortés-Guzmán, F., Molecular recognition between DNA and a copper-based anticancer complex. *Physical Chemistry Chemical Physics* **2012**, *14* (44), 15539-15546.
- (16) Galindo-Murillo, R.; García-Ramos, J. C.; Ruiz-Azuara, L.; Cheatham, T. E.; Cortés-Guzmán, F., Intercalation processes of copper complexes in DNA. *Nucleic Acids Res.* **2015**, *43* (11), 5364-5376.
- (17) Vanquelef, E.; Simon, S.; Marquant, G.; Garcia, E.; Klimerak, G.; Delepine, J. C.; Cieplak, P.; Dupradeau, F.-Y., RED Server: a web service for deriving RESP and ESP charges and building force field libraries for new molecules and molecular fragments. *Nucleic Acids Res.* **2011**, *39* (suppl\_2), W511-W517.
- (18) Bayly, C. I.; Cieplak, P.; Cornell, W.; Kollman, P. A., A well-behaved electrostatic potential based method using charge restraints for deriving atomic charges: the RESP model. *J. Phys. Chem.* **1993**, *97* (40), 10269-10280.
- (19) Henchman, R. H.; Essex, J. W., Generation of OPLS-like charges from molecular electrostatic potential using restraints. *J. Comput. Chem.* **1999**, *20* (5), 483-498.
- (20) Galindo-Murillo, R.; Bergonzo, C.; Cheatham III, T. E., Molecular modeling of nucleic acid structure: Setup and analysis. *Curr. Protoc. Nucleic Acid Chem.* **2014**, *56* (1), 7.10. 1-7.10. 21.
- (21) Jorgensen, W. L.; Chandrasekhar, J.; Madura, J. D.; Impey, R. W.; Klein, M. L., Comparison of simple potential functions for simulating liquid water. *J. Chem. Phys.* **1983**, *79* (2), 926-935.
- (22) Kůhrová, P.; Otyepka, M.; Šponer, J. í.; Banáš, P., Are waters around RNA more than just a solvent?—an insight from molecular dynamics simulations. *J. Chem. Theory Comput.* **2014**, *10* (1), 401-411.
- (23) Pantatosaki, E.; Papadopoulos, G. K., Binding Dynamics of siRNA with Selected Lipopeptides: A Computer-Aided Study of the Effect of Lipopeptides' Functional Groups and Stereoisomerism. *J. Chem. Theory Comput.* **2020**, *16* (6), 3842-3855.
- (24) Berendsen, H. J.; Postma, J. v.; van Gunsteren, W. F.; DiNola, A.; Haak, J. R., Molecular dynamics with coupling to an external bath. *J. Chem. Phys.* **1984**, *81* (8), 3684-3690.
- (25) Bussi, G.; Donadio, D.; Parrinello, M., Canonical sampling through velocity rescaling. *J. Chem. Phys.* **2007**, *126* (1), 014101.
- (26) Hess, B.; Bekker, H.; Berendsen, H. J.; Fraaije, J. G., LINCS: a linear constraint solver for molecular simulations. *J. Comput. Chem.* **1997**, *18* (12), 1463-1472.
- (27) Hess, B., P-LINCS: A parallel linear constraint solver for molecular simulation. *J. Chem. Theory Comput.* **2008**, *4* (1), 116-122.
- (28) Essmann, U.; Perera, L.; Berkowitz, M. L.; Darden, T.; Lee, H.; Pedersen, L. G., A smooth particle mesh Ewald method. *J. Chem. Phys.* **1995**, *103* (19), 8577-8593.
- (29) Lavery, R.; Moakher, M.; Maddocks, J. H.; Petkeviciute, D.; Zakrzewska, K., Conformational analysis of nucleic acids revisited: Curves. *Nucleic Acids Res.* **2009**, *37* (17), 5917-5929.
- (30) Humphrey, W.; Dalke, A.; Schulten, K., VMD: visual molecular dynamics. *J. Mol. Graph.* **1996**, *14* (1), 33-38.
- (31) Sechrist III, J. A., Nucleoside and Nucleotide Nomenclature. *Curr. Protoc. Nucleic Acid Chem.* **2000**, (1), A. 1D. 1-A. 1D. 3.

- (32) Zgarbová, M.; Otyepka, M.; Sponer, J.; Lankas, F.; Jurečka, P., Base pair fraying in molecular dynamics simulations of DNA and RNA. *J. Chem. Theory Comput.* **2014**, *10* (8), 3177-3189.
- (33) Berg, J. M.; Tymoczko, J. L.; Stryer, L., Biochemistry. 5th Edition. *Biochemistry. 5th Edition*, New York: *W H Freeman* **2002**.

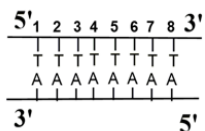
## Supplementary Schemes



**Scheme S1.** The absolute configurations of *endo* and *exo* isomers of the Diels-Alder product 3a.<sup>6</sup>



**21-6, 7:** "21" indicates the number of base pairs for this sequence, and "6, 7" shows the position of G-C pair.

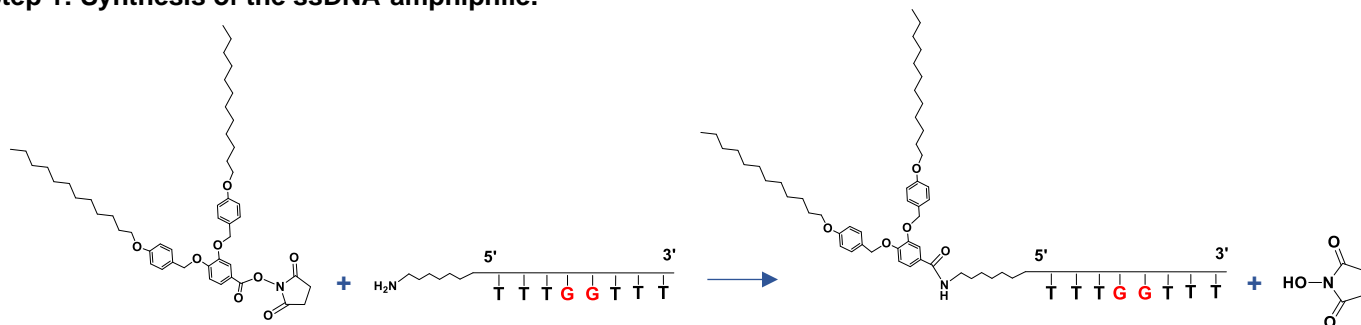


**8:** "8" indicates the number of base pairs for this sequence, and no indication for position of G-C pair means there are no G-C pairs in this sequence.

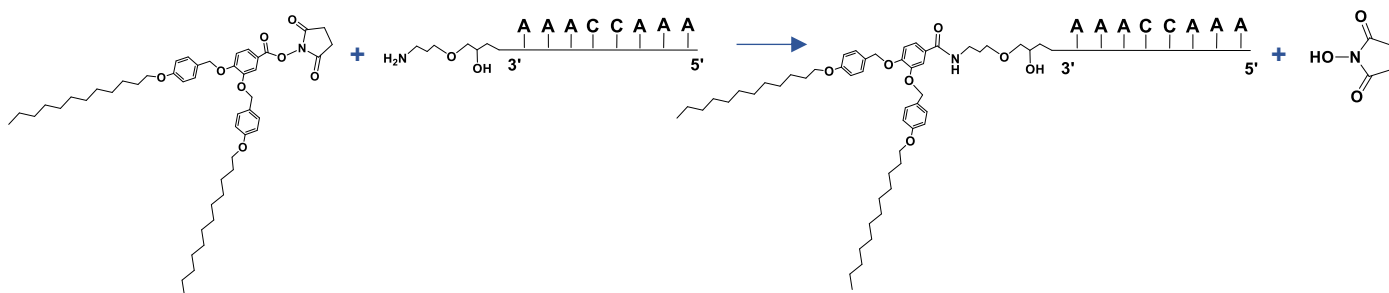
**Scheme S2.** Examples for designating DNA sequences used in this study.



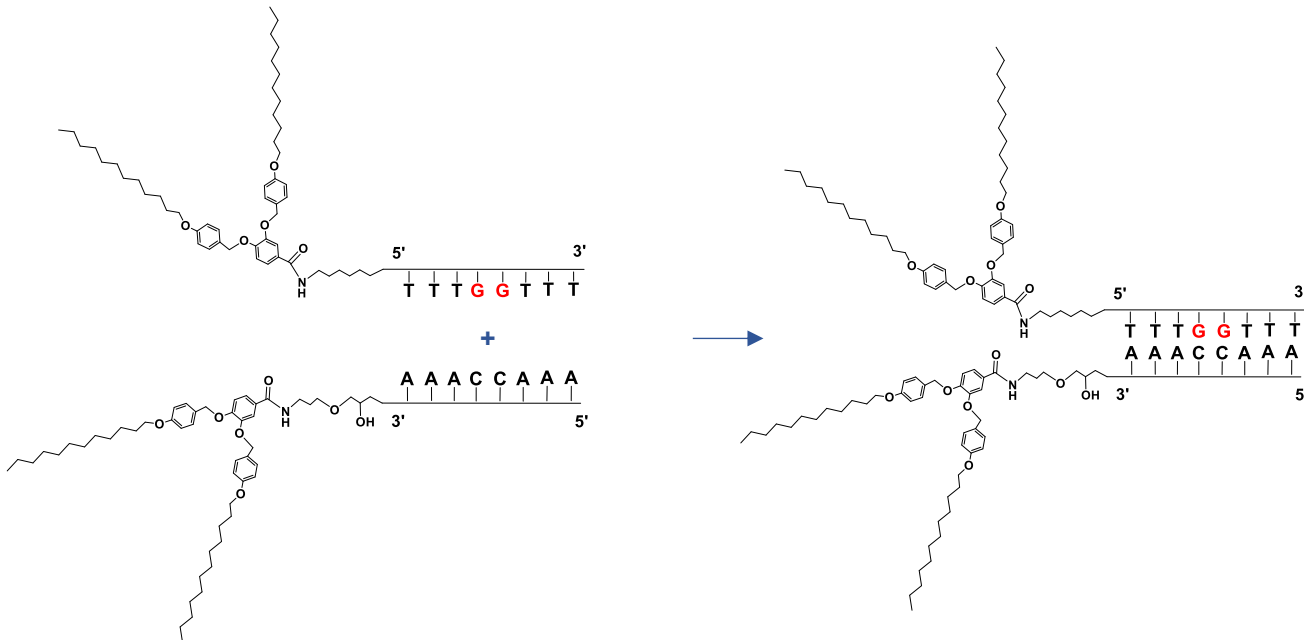
### Step 1: Synthesis of the ssDNA-amphiphile.



### Step 2: Synthesis of the complementary ssDNA-amphiphile.



### Step 3: Hybridization of the ssDNA-amphiphiles.

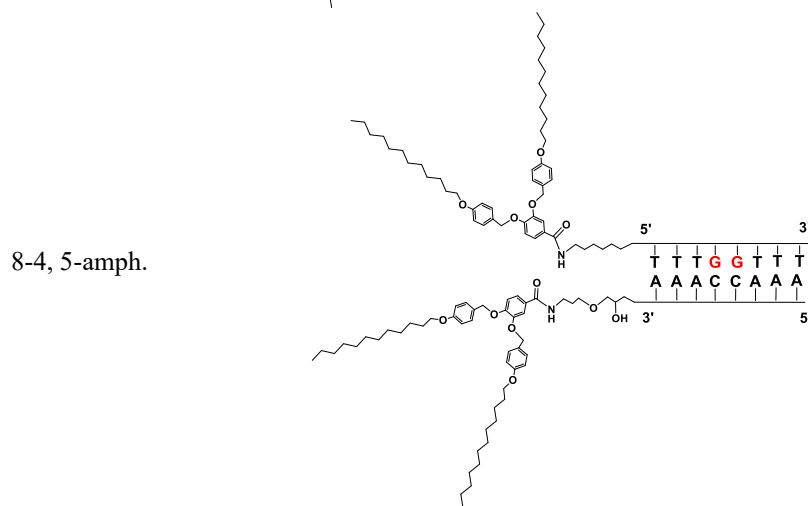
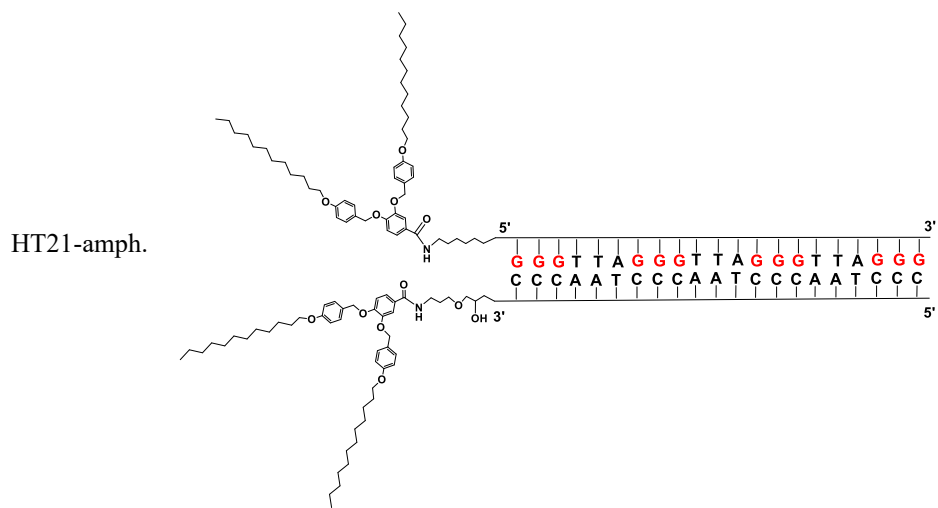
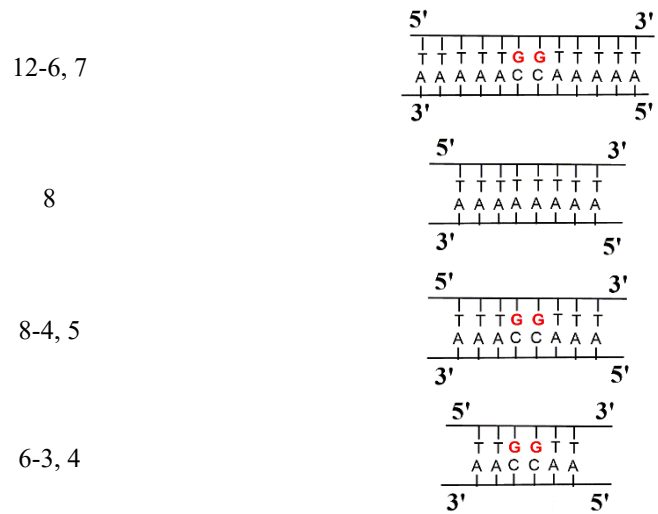


**Scheme S3.** Typical procedure for the synthesis and hybridization of the dsDNA-amphiphiles.

## Supplementary Tables

**Table S1.** dsDNA sequences employed in this work.

Name	Sequence
HT21	<pre> 5'-----3' G G G T T A G G G T T A G G G T T A G G G C C C A A T C C C A A T C C C A A T C C C </pre>
21	<pre> 5'-----3' T A </pre>
21-6	<pre> 5'-----3' T T T T T G T T T T T T T T T T T T T T T T A A A A A C A A A A A A A A A A A A A A A A </pre>
21-6, 7	<pre> 5'-----3' T T T T T G G T T T T T T T T T T T T T T T T A A A A A C C A A A A A A A A A A A A A A A A </pre>
21-6, 7, 8	<pre> 5'-----3' T T T T T G G G T T T T T T T T T T T T T T T T A A A A A C C C A A A A A A A A A A A A A A A A </pre>
21-6, 7, 8, 9	<pre> 5'-----3' T T T T T G G G G T T T T T T T T T T T T T T T T T A A A A A C C C C A A A A A A A A A A A A A A A A </pre>
21-6, 16	<pre> 5'-----3' T T T T T G T T T T T T T T T T G T T T T T T T A A A A A C A A A A A A A A A A C A A A A A A A </pre>
21-10, 11	<pre> 5'-----3' T T T T T T T T T T G G T T T T T T T T T T T T T T A A A A A A A A A C C A A A A A A A A A A A A A A </pre>
21-15, 16	<pre> 5'-----3' T T T T T T T T T T T T T T T T G G T T T T T T T T A A A A A A A A A A A A A A A A C C A A A A A A </pre>
21-18, 19	<pre> 5'-----3' T T T T T T T T T T T T T T T T T T G G T T T T A A A A A A A A A A A A A A A A A C C A A A A </pre>
21-20, 21	<pre> 5'-----3' T T T T T T T T T T T T T T T T T T G G T T T T A C C </pre>


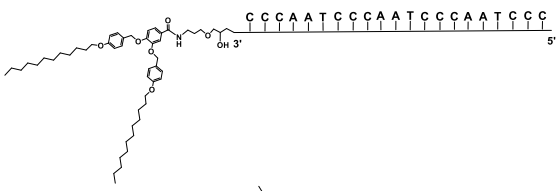
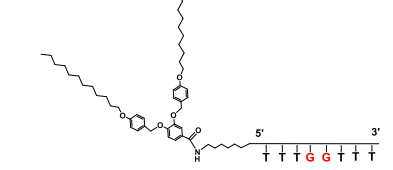
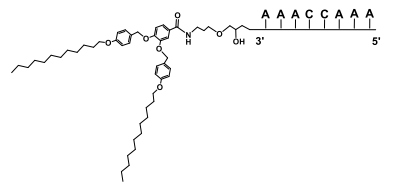


**Table S2.** Molecular weight of dmbipy-Cu.

Complex	Calculated	Measured <sup>[a]</sup>
dmbipy-Cu	308.02 (dmbipy-CuNO <sub>3</sub> <sup>+</sup> )	309.0

[a] Mass observed in MALDI-TOF MS analysis.

**Table S3.** Molecular weight of ssDNA-amphiphiles.

Complex	Calculated	Measured <sup>[a]</sup>
	7517.5	7525.9
	7096.2	7060.0
	3285.8	3290.6
	3291.8	3298.2

[a] Mass observed in MALDI-TOF MS analysis.

**Table S4.** The sequence of bases along the strands of the dsDNA molecules modeled in this study; the numbering of bases and base pairs are also shown.

<b>“21” sequence</b>		<b>Strand 5' to 3'</b>		<b>Strand 3' to 5'</b>	
<b>Number of nucleotide pair or base pair</b>	<b>Base number</b>	<b>Base type</b>	<b>Base type</b>	<b>Base number</b>	
1	1	T	A	42	
2	2	T	A	41	
3	3	T	A	40	
4	4	T	A	39	
5	5	T	A	38	
6	6	T	A	37	
7	7	T	A	36	
8	8	T	A	35	
9	9	T	A	34	
10	10	T	A	33	
11	11	T	A	32	
12	12	T	A	31	
13	13	T	A	30	
14	14	T	A	29	
15	15	T	A	28	
16	16	T	A	27	
17	17	T	A	26	
18	18	T	A	25	
19	19	T	A	24	
20	20	T	A	23	
21	21	T	A	22	
<b>“21-10, 11” sequence</b>		<b>Strand 5' to 3'</b>		<b>Strand 3' to 5'</b>	
<b>Number of nucleotide pair or base pair</b>	<b>Base number</b>	<b>Base type</b>	<b>Base type</b>	<b>Base number</b>	
1	1	T	A	42	
2	2	T	A	41	
3	3	T	A	40	
4	4	T	A	39	
5	5	T	A	38	
6	6	T	A	37	
7	7	T	A	36	
8	8	T	A	35	
9	9	T	A	34	
10	10	G	C	33	
11	11	G	C	32	
12	12	T	A	31	
13	13	T	A	30	
14	14	T	A	29	
15	15	T	A	28	
16	16	T	A	27	

17	17	T	A	26
18	18	T	A	25
19	19	T	A	24
20	20	T	A	23
21	21	T	A	22

**Table S5.** Computed and experimental structural observables for the dmbipy-Cu; for the notation of atoms see Figure S17.

Structural observable	Crystallographic value <sup>9</sup> (degrees)	Computed value “21” (degrees)	Computed value “21-10, 11” (degrees)
N2-Cu-N3 angle	83.4	84.8 ± 1.5	85.0 ± 1.5
Cu-N2-C4 angle	127.7	127.9 ± 2.5	128.3 ± 2.5
Cu-N2-C8 angle	113.1	108.6 ± 2.0	108.3 ± 2.0
Cu-N3-C10 angle	127.7	128.3 ± 2.5	128.6 ± 2.4
Cu-N3-C14 angle	113.1	108.5 ± 1.9	108.3 ± 1.9
C7-C8-C14-C13 dihedral angle	3.3	-0.6 ± 7.8	0.4 ± 7.9
N2-C8-C14-N3 dihedral angle	4.0	0.1 ± 6.1	0.4 ± 6.1

**Table S6.** Melting temperature of different sequences as a function of DNA concentration in phosphate buffer.

Concentration (μM)	Melting temperature (° C) <sup>[a]</sup>			
	“8-4,5”	“8”	HT21	st-DNA
3	16.02 ± 0.01	4.00 ± 0.01	66.01 ± 0.01	85.76 ± 0.56
15	23.97 ± 1.10	12.02 ± 0.01	66.82 ± 0.56	87.03 ± 0.01

[a] Data are shown as mean ± SD (n=3).

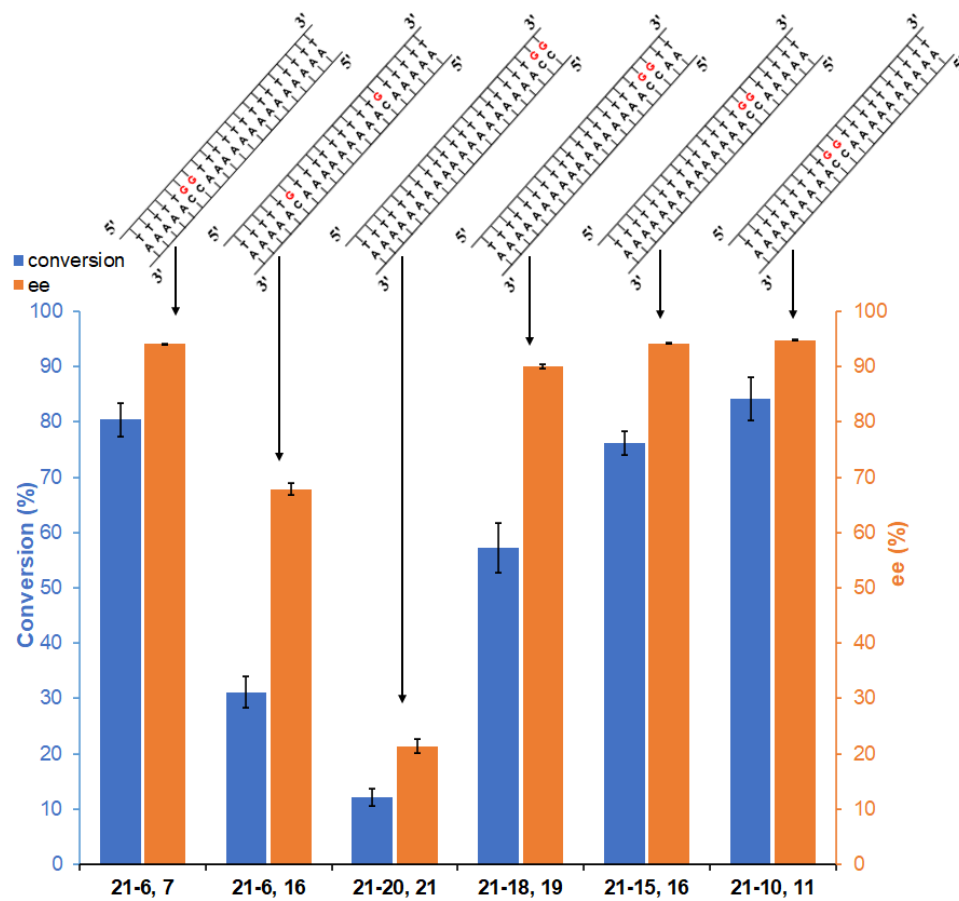
**Table S7.** Conversion and ee% for Diels-Alder reaction catalyzed by D-DNA and/or L-DNA with dmbipy-Cu.<sup>[a]</sup>

Entry	D-DNA ( $\mu\text{M}$ )	L-DNA ( $\mu\text{M}$ )	Conversion (%)	<i>endo/exo</i>	ee (%) <sup>[b]</sup>
1	50	--	71	99/1	95
2	--	50	63	99/1	-95
3	25	25	45	98/2	-2

[a] Same reaction conditions as in Figure 1.

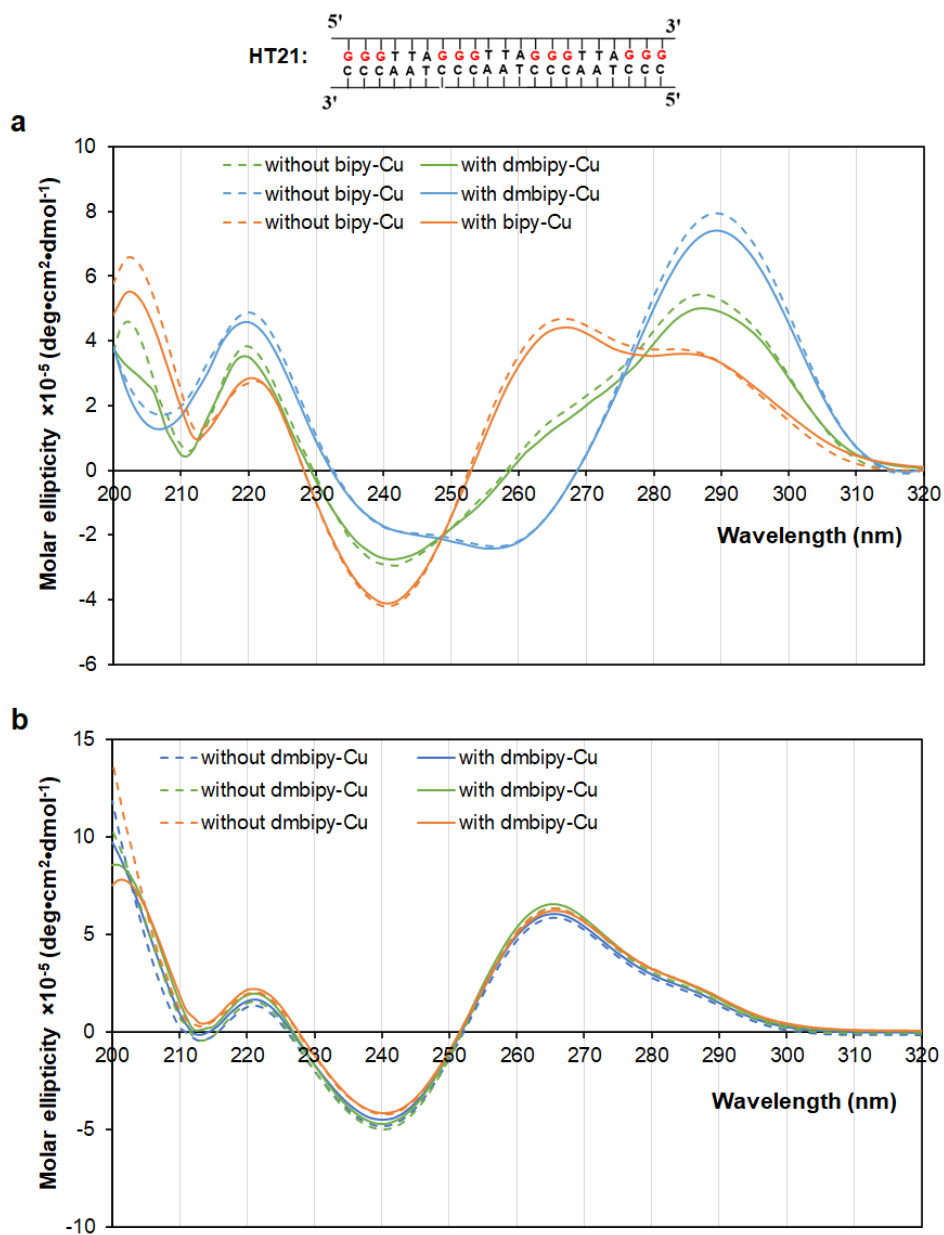
[b] ee% = (moles of *Si-endo* – moles of *Re-endo*) / (moles of *Si-endo* + moles of *Re-endo*)  $\times$  100%.

## Supplementary Figures

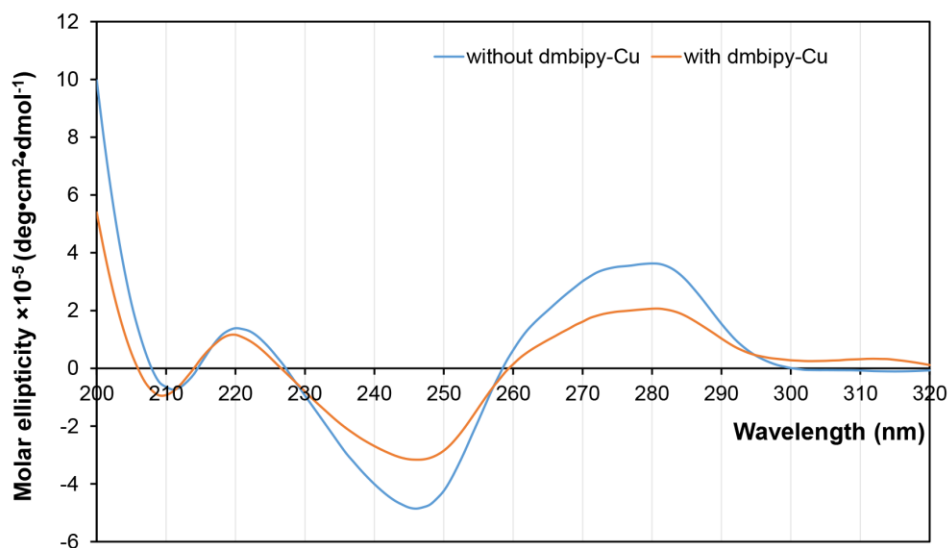


**Figure S1.** Conversion and ee% for Diels-Alder reaction catalyzed by 21-base pair dsDNA sequences containing two G•C pairs at different positions with dmbipy-Cu. Same reaction conditions as in Figure 1.

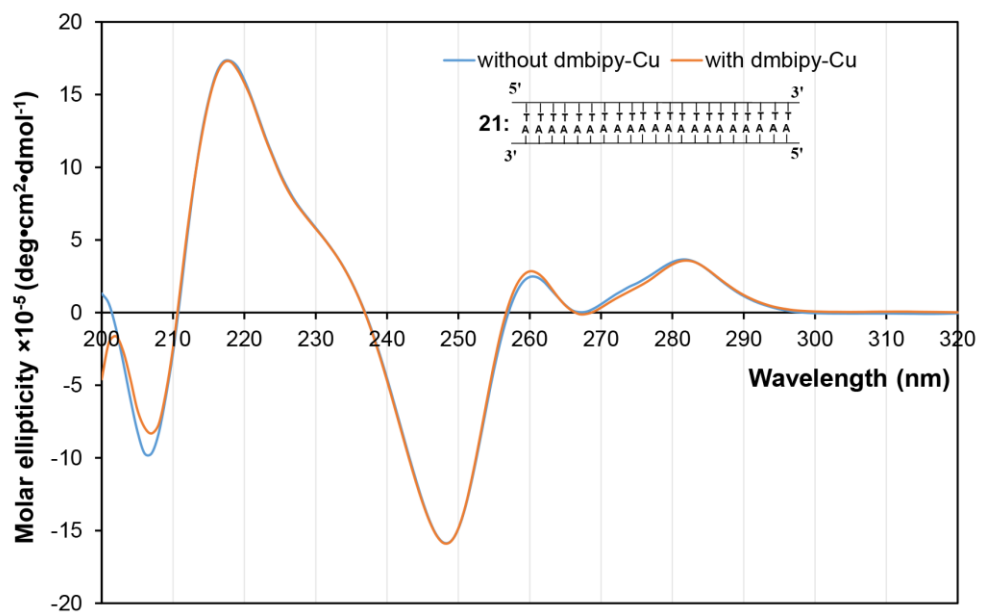




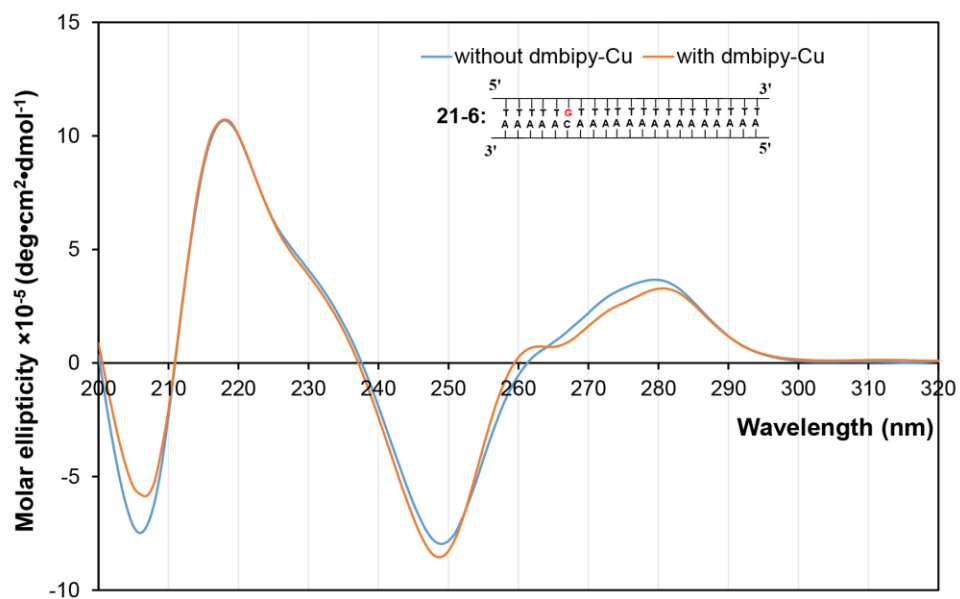
**Figure S2.** (a) CD spectra of HT21 sequence (50  $\mu$ M, in 20 mM MOPS buffer, pH 6.5) in the absence or presence of dmbipy-Cu (1 eq.). Spectra are shown from three independent experiments. (b) CD spectra of HT21 sequence (50  $\mu$ M, in 20 mM MOPS buffer, pH 6.5) stabilized by 0.1 M NaCl in the absence or presence of dmbipy-Cu (1 eq.). Spectra are shown from three independent experiments.



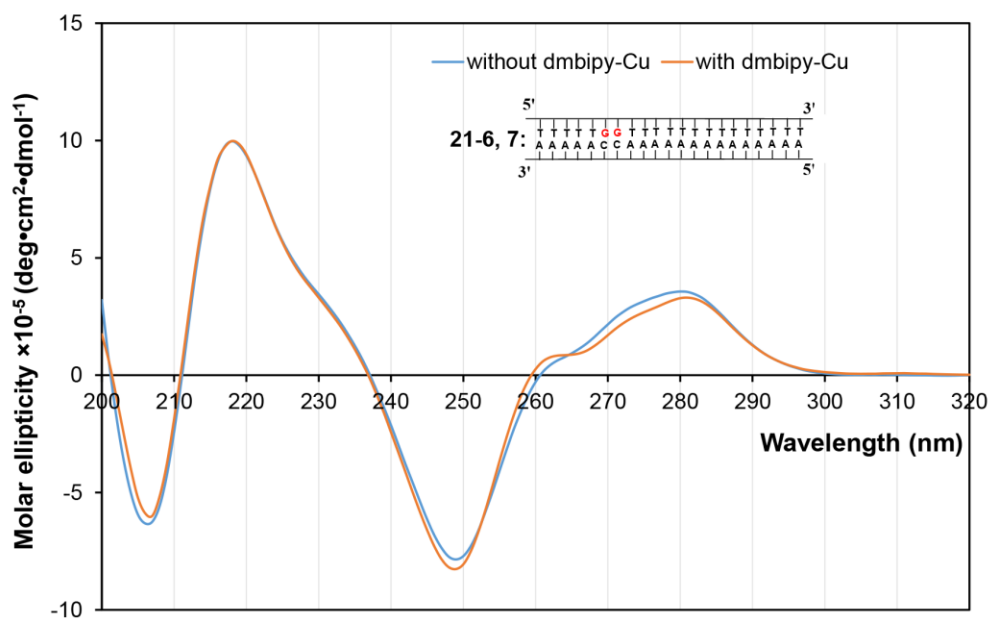
**Figure S3.** CD spectra of st-DNA (1.05 mM base pairs, in 20 mM MOPS buffer, pH 6.5) in the absence or presence of dmbipy-Cu (1 eq.).



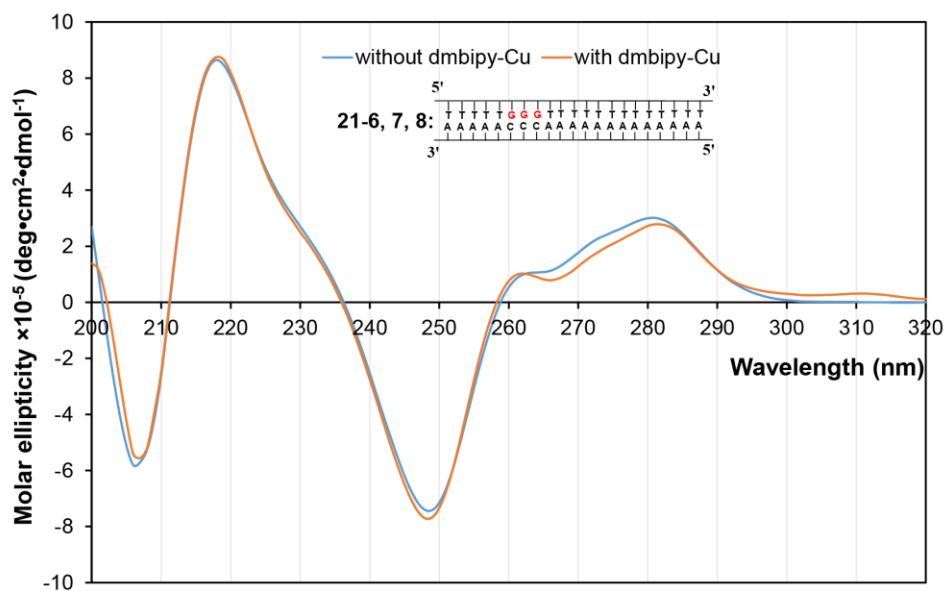
**Figure S4.** CD spectra of “21” sequence (50  $\mu$ M, in 20 mM MOPS buffer, pH 6.5) in the absence or presence of dmbipy-Cu (1 eq.).



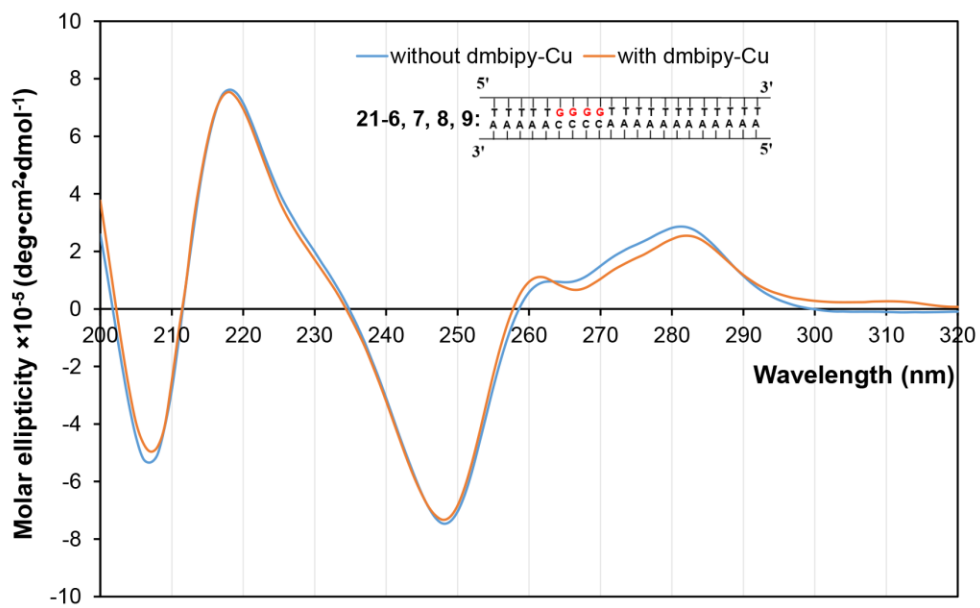
**Figure S5.** CD spectra of "21-6" sequence (50  $\mu\text{M}$ , in 20 mM MOPS buffer, pH 6.5) in the absence or presence of dmbipy-Cu (1 eq.).



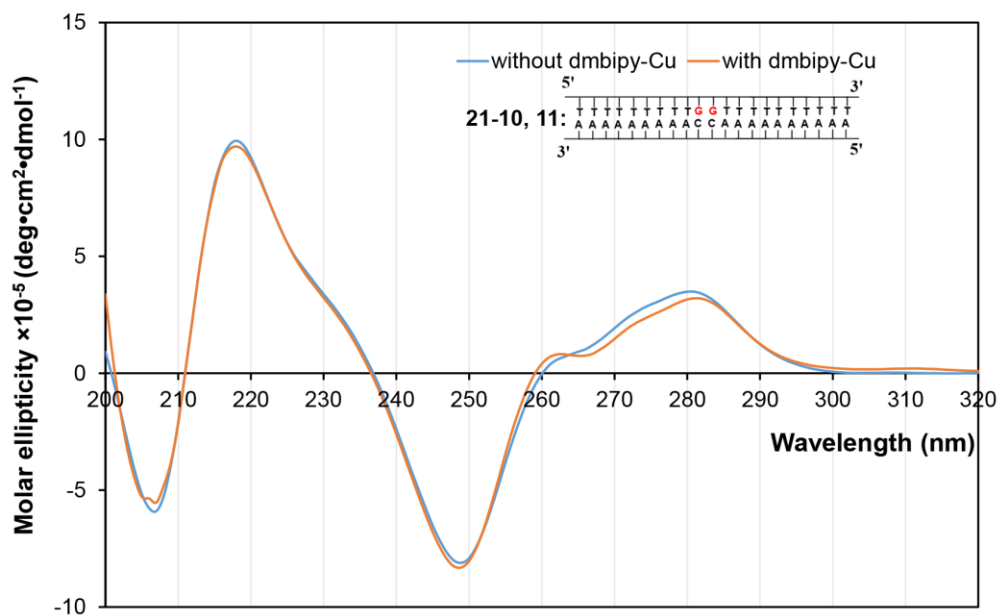
**Figure S6.** CD spectra of "21-6, 7" sequence (50  $\mu\text{M}$ , in 20 mM MOPS buffer, pH 6.5) in the absence or presence of dmbipy-Cu (1 eq.).



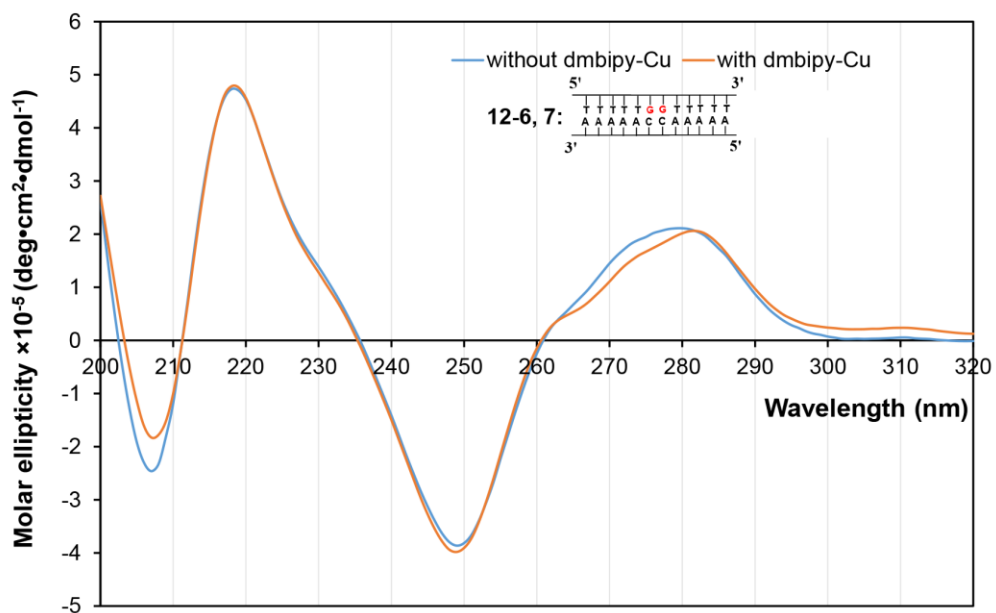
**Figure S7.** CD spectra of “21-6, 7, 8” sequence (50  $\mu$ M, in 20 mM MOPS buffer, pH 6.5) in the absence or presence of dmbipy-Cu (1 eq.).



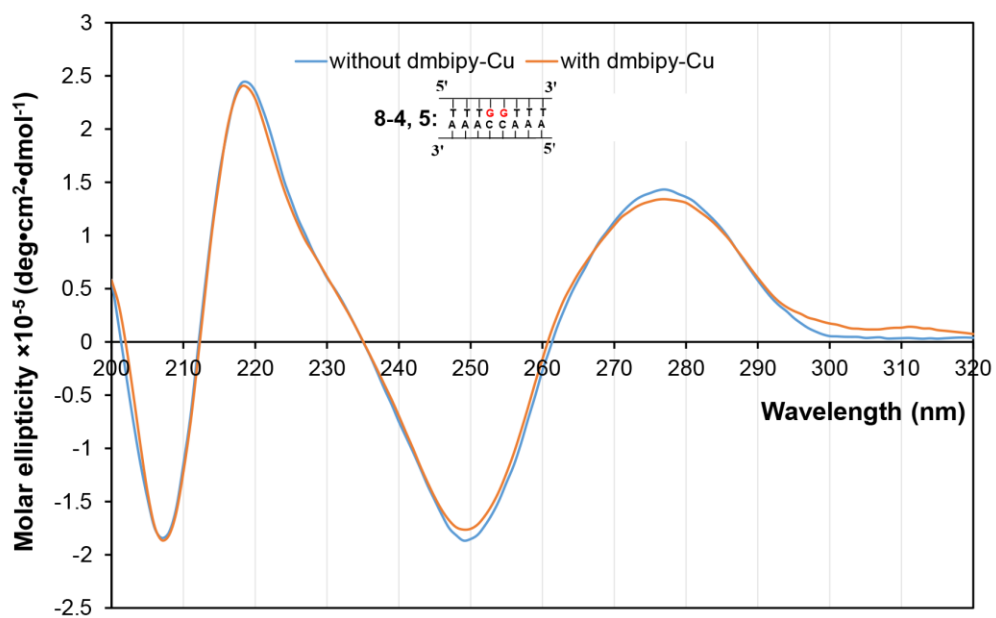
**Figure S8.** CD spectra of “21-6, 7, 8, 9” sequence (50  $\mu$ M, in 20 mM MOPS buffer, pH 6.5) in the absence or presence of dmbipy-Cu (1 eq.).



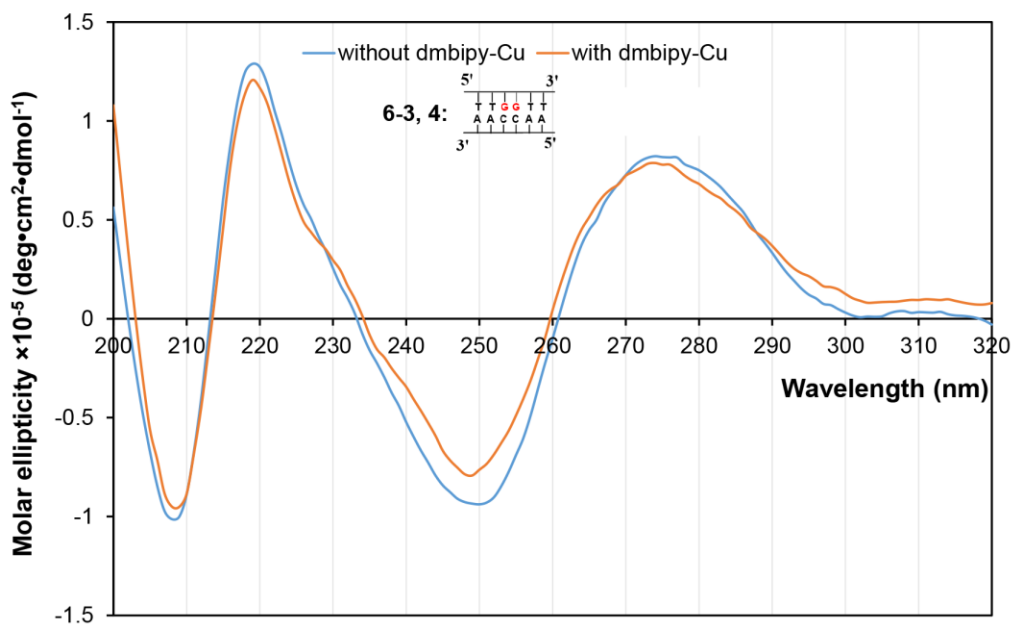
**Figure S9.** CD spectra of "21-10, 11" sequence (50  $\mu$ M, in 20 mM MOPS buffer, pH 6.5) in the absence or presence of dmbipy-Cu (1 eq.).



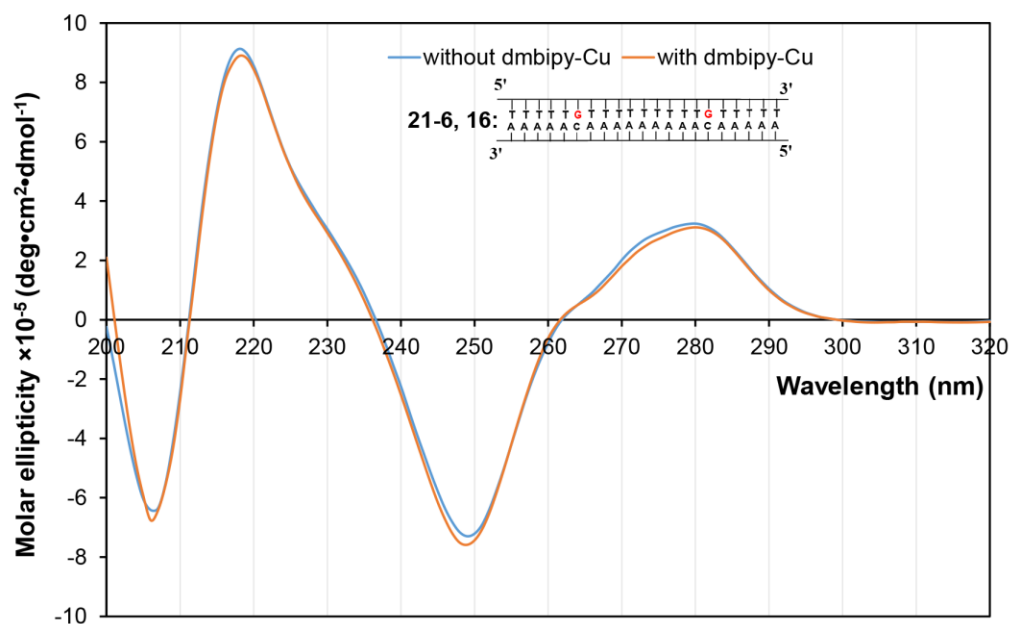
**Figure S10.** CD spectra of "12-6, 7" sequence (50  $\mu$ M, in 20 mM MOPS buffer, pH 6.5) in the absence or presence of dmbipy-Cu (1 eq.).



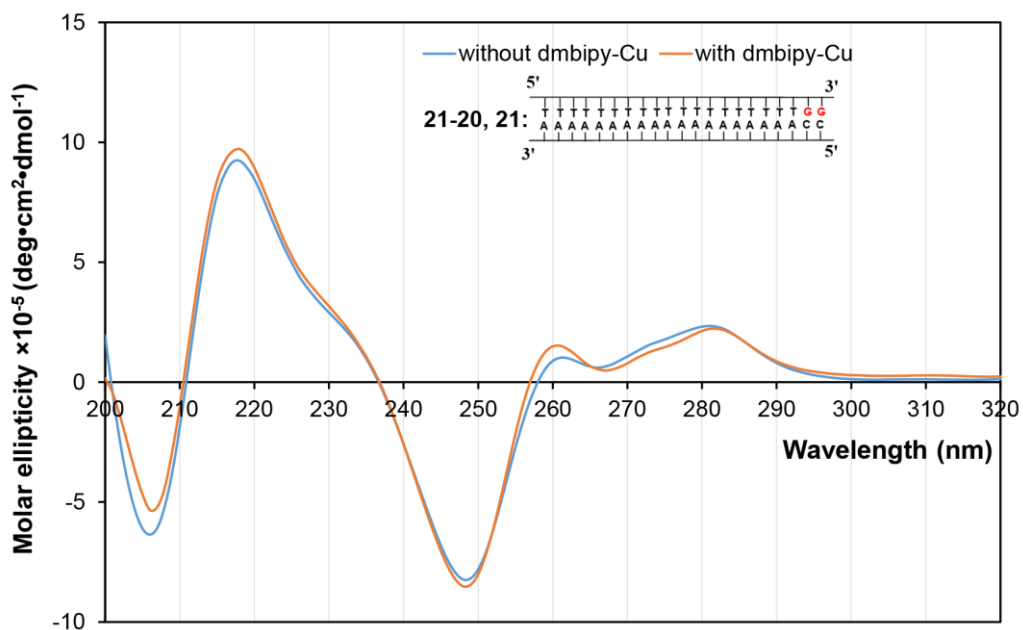
**Figure S11.** CD spectra of "8-4, 5" sequence (50  $\mu\text{M}$ , in 20 mM MOPS buffer, pH 6.5) in the absence or presence of dmbipy-Cu (1 eq.).



**Figure S12.** CD spectra of "6-3, 4" sequence (50  $\mu\text{M}$ , in 20 mM MOPS buffer, pH 6.5) in the absence or presence of dmbipy-Cu (1 eq.).



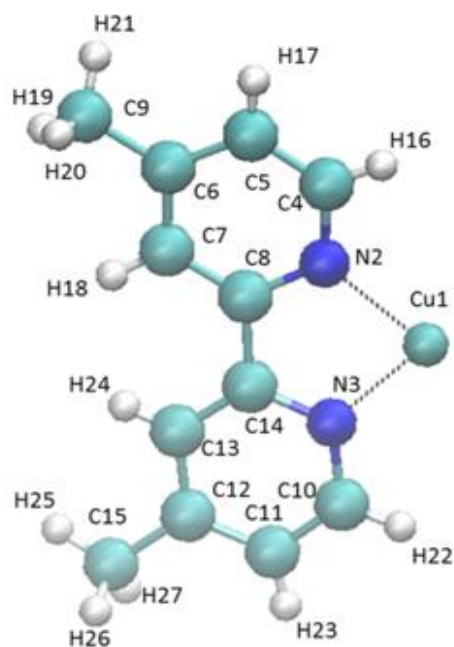
**Figure S13.** CD spectra of "21-6, 16" sequence (50  $\mu\text{M}$ , in 20 mM MOPS buffer, pH 6.5) in the absence or presence of dmbipy-Cu (1 eq.).



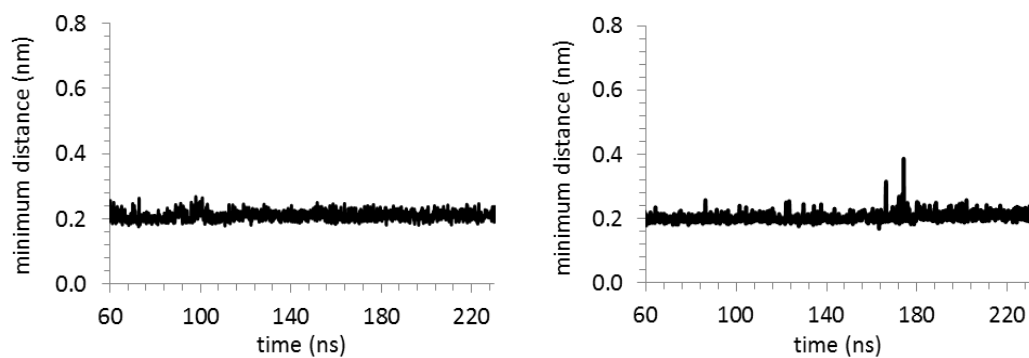
**Figure S14.** CD spectra of "21-20, 21" sequence (50  $\mu\text{M}$ , in 20 mM MOPS buffer, pH 6.5) in the absence or presence of dmbipy-Cu (1 eq.).



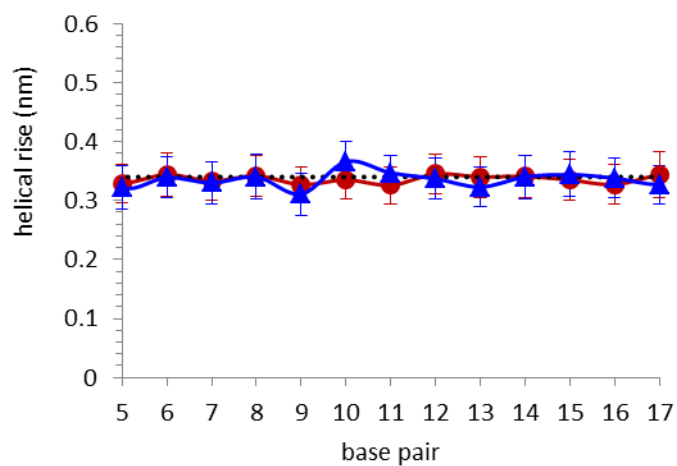




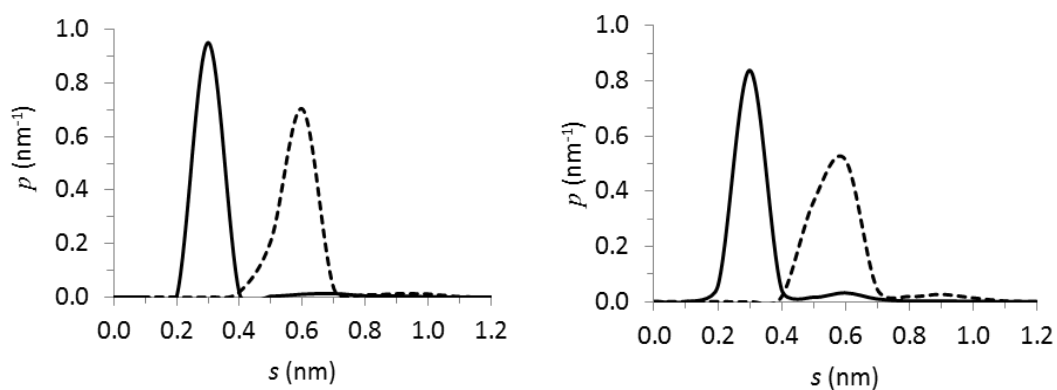
**Figure S17.** Atoms notation in the modeled dmbipy-Cu complex.



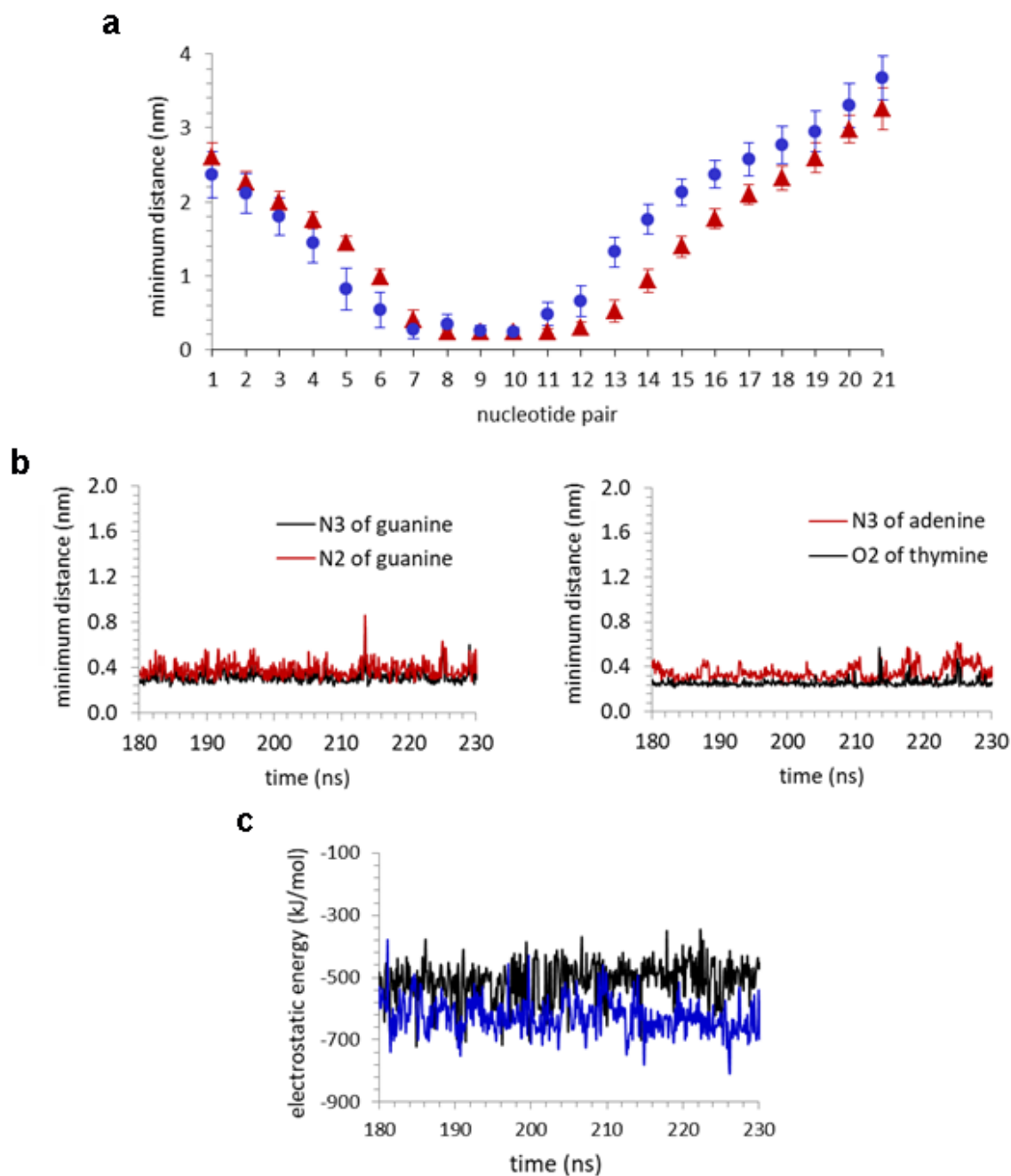
**Figure S18.** Time evolution of the distance between the DNA and the dmbipy-Cu, computed as the minimum distance of all the DNA atoms with all the dmbipy-Cu atoms, over the last 170 ns of the equilibrated MD trajectory for “21” (left) and “21-10, 11” (right); distances below 0.4 nm denote bound molecules.



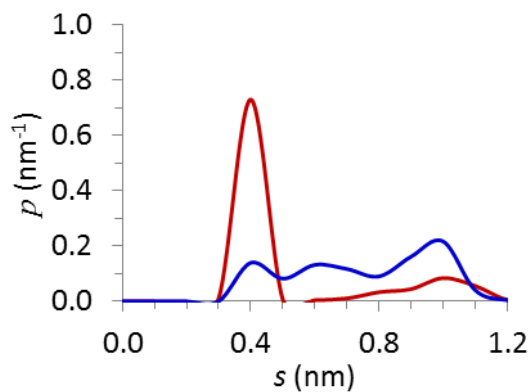
**Figure S19.** Rise per base pair along the helix axis computed over the entire MD trajectory, for “21” (red) and “21-10, 11” (blue); the crystallographic value of the rise per base pair<sup>53</sup> is also depicted (dotted line) for comparison.



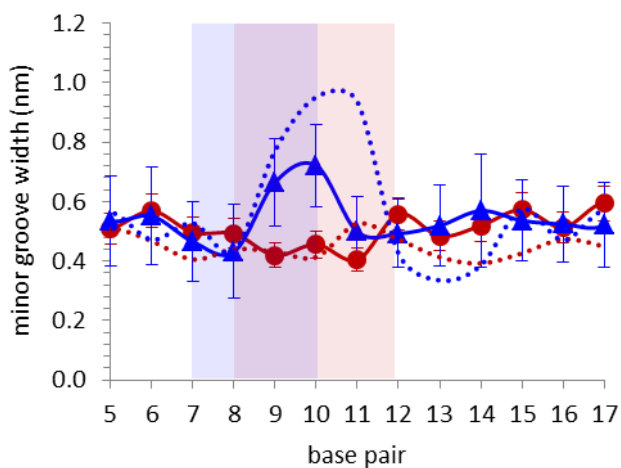
**Figure S20.** Probability density functions of finding the dmbipy-Cu at various distances from the minor (continuous line), or major (dashed line), groove base atoms (see text), for „21“ (left) and „21-10, 11“ (right), computed over the last 170 ns of the equilibrated MD trajectory.



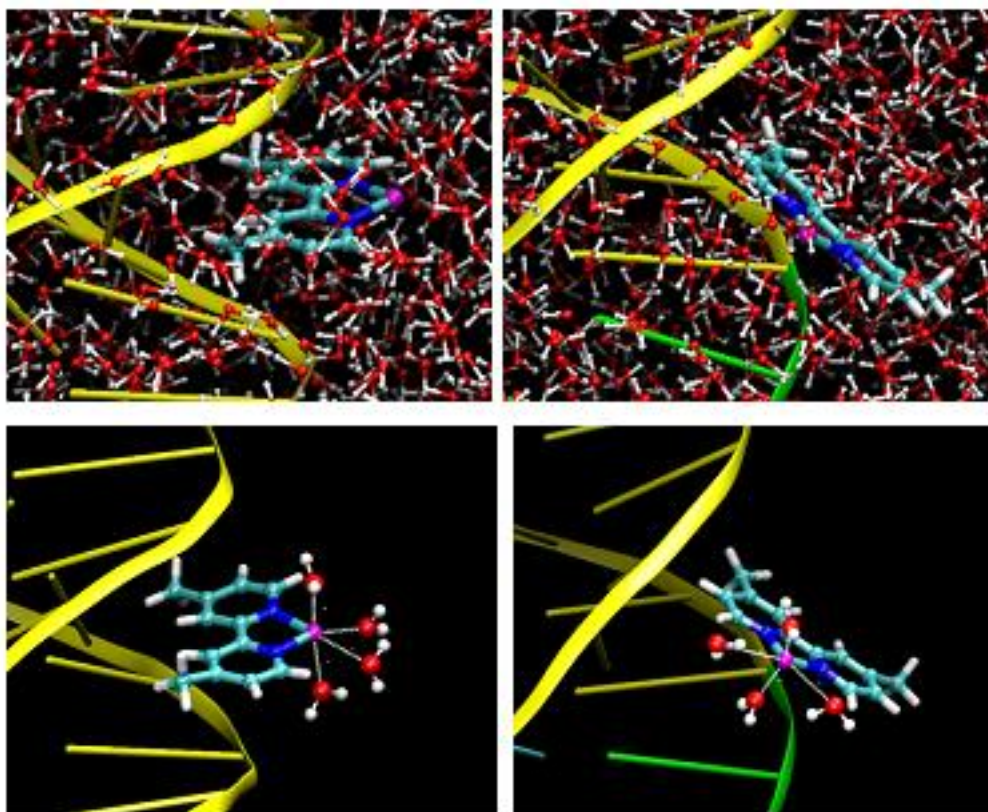
**Figure S21.** (a) Minimum distance between the dmbipy-Cu and each of the 21 DNA nucleotide pairs, computed over the equilibrated MD trajectory for “21” (red) and “21-10, 11” (blue). The numbering of nucleotide pairs for the two sequences can be seen in Table S4. (b) Minimum distances between the dmbipy-Cu and the electronegative minor groove atoms N2 and N3 of guanines (left), and N3 of adenine and O2 of thymine residing in the proximity of the G•C pairs (right); computations over the last 40 ns of the MD trajectory for the “21-10, 11” system. (c) Electrostatic energy between the dmbipy-Cu and the DNA for both the “21” (black) and the “21-10, 11” (blue) systems, computed over the last 40 ns of the MD trajectory for the “21-10, 11” system.



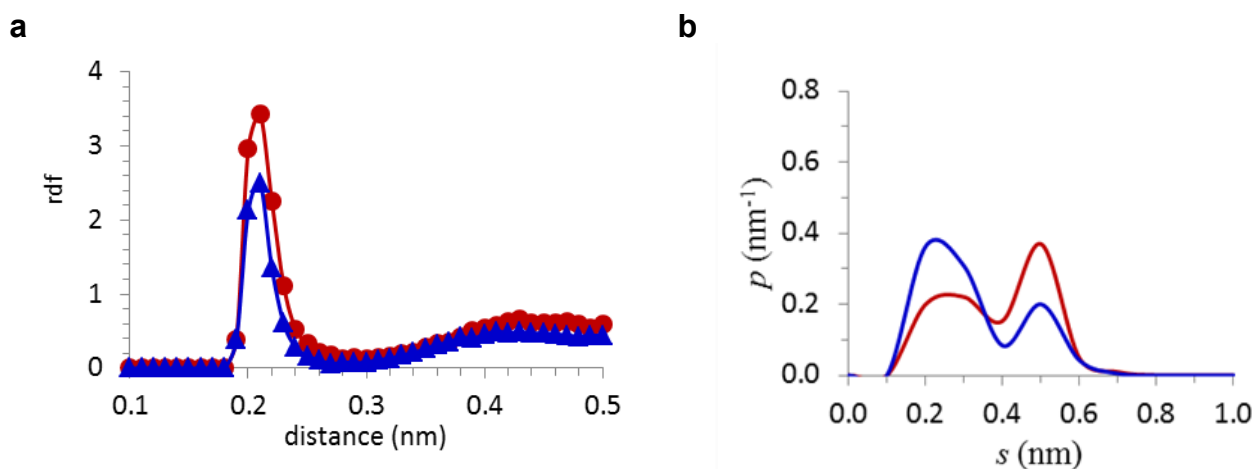
**Figure S22.** Probability density functions of finding the pyridine methyl carbon C9 of the dmbipy-Cu at various distances from the minor groove base atoms (see text) in “21” (red) and “21-10, 11” (blue), computed over the last 170 ns of the equilibrated MD trajectory. For the notation of carbon atom see Figure S17.



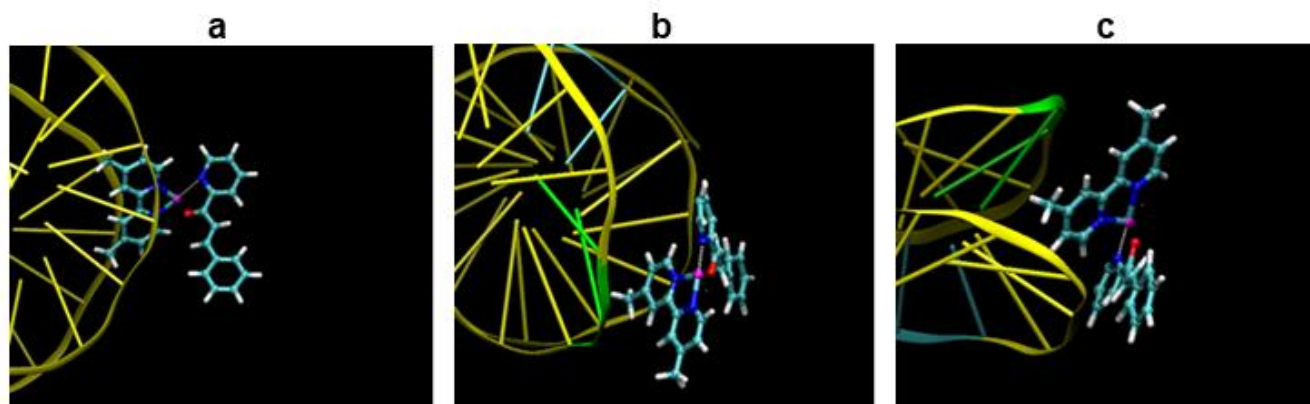
**Figure S23.** Minor groove width along the DNA helix for the “21” (red) and “21-10, 11” (blue), computed over the entire MD trajectory (continuous lines); the minor groove width for the initial DNA structures is also shown (dotted lines). Shaded rectangles denote the nucleotide pairs whereat the dmbipy-Cu binds in “21” (light red) and “21-10, 11” (light blue).



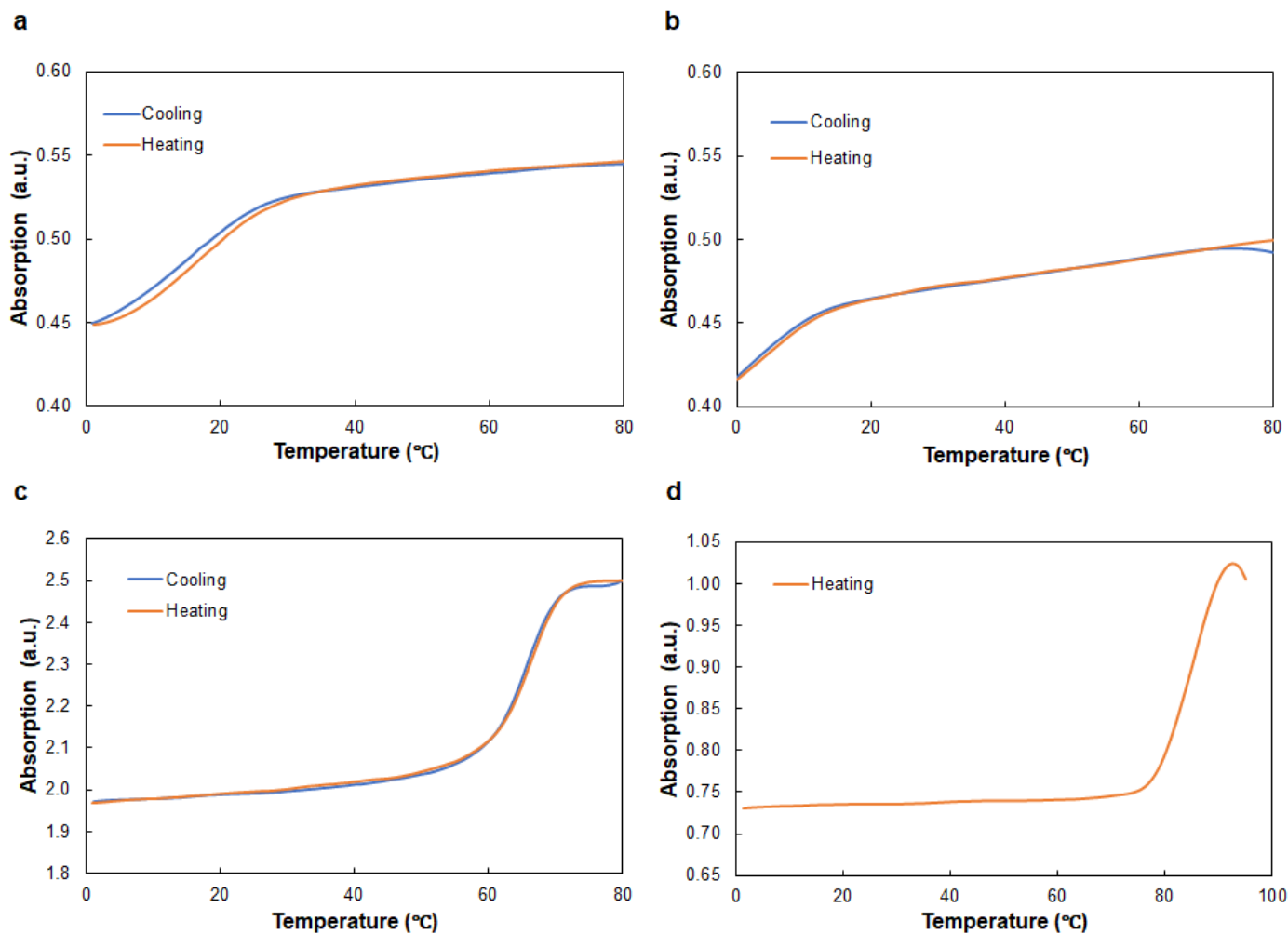
**Figure S24.** Indicative configurations rendered from the MD trajectory of the dmbipy-Cu binding to the DNA in “21” (left) and “21-10, 11” (right), depicting also: the water molecules surrounding the complex (top); only the first-shell coordination waters around the copper atom of the dmbipy-Cu at the square-planar equatorial and axial positions (bottom). Color code for the dmbipy-Cu and waters: Cu (magenta), N (blue), C (cyan), H (white), O (red); color code for the DNA: guanine (green), cytosine (cyan), adenine and thymine (yellow).



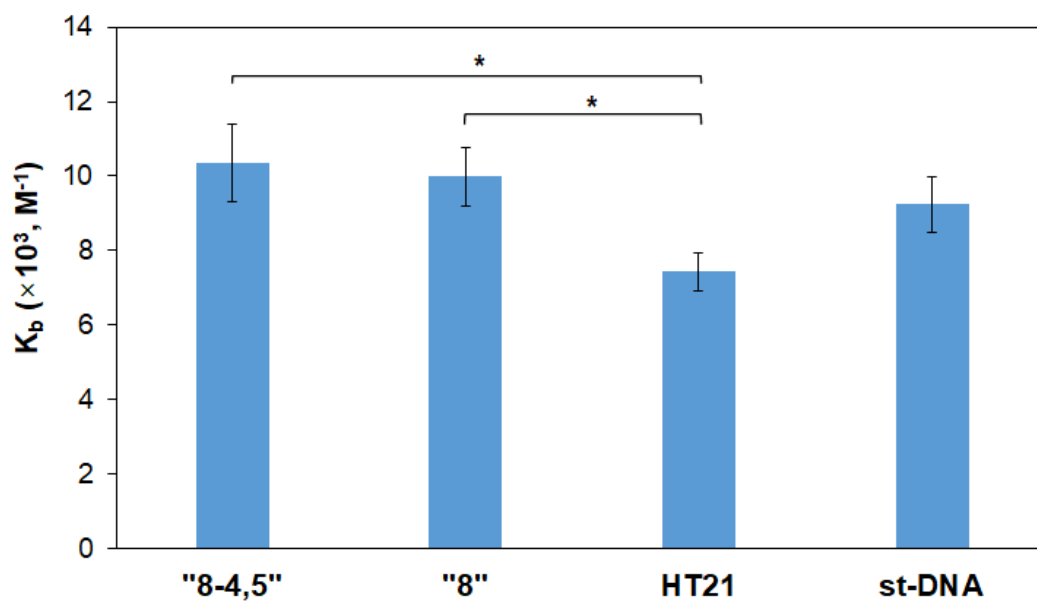
**Figure S25.** (a) Radial distribution function of water oxygens with respect to the copper atom, and (b) probability density functions of finding the copper atom at various distances from the oxygen atoms of the DNA phosphate groups (b), in “21” (red) and “21-10, 11” (blue), computed over the equilibrated MD trajectory.



**Figure S26.** The reactant [1a], added by following the bidentate coordination pattern of the enone to the copper atom of the dmbipy-Cu as shown in Figure 2 (e), is depicted in (a) for “21”, and (b, c) for “21-10, 11” (b, c are rotated views of the same configuration). The configurations depicted in (a), (b) and (c) correspond to the ones shown in Figure 2 (f), (g) and (h), with only difference being that the reactant [1a] is rotated by 180°, i.e., in (a) the *Si*-face is shown (while in Figure 2 (f) the view is down the *Re*-face) and in (b) and (c) the *Re*-face is facing the DNA (while in Figure 2 (g) and (h) the *Si*-face is facing the DNA). Water molecules in the rendered pictures are omitted for clarity. Color code for the dmbipy-Cu and reactant [1a]: Cu (magenta), N (blue), C (cyan), H (white), O (red); color code for the DNA: guanine (green), cytosine (cyan), adenine and thymine (yellow).

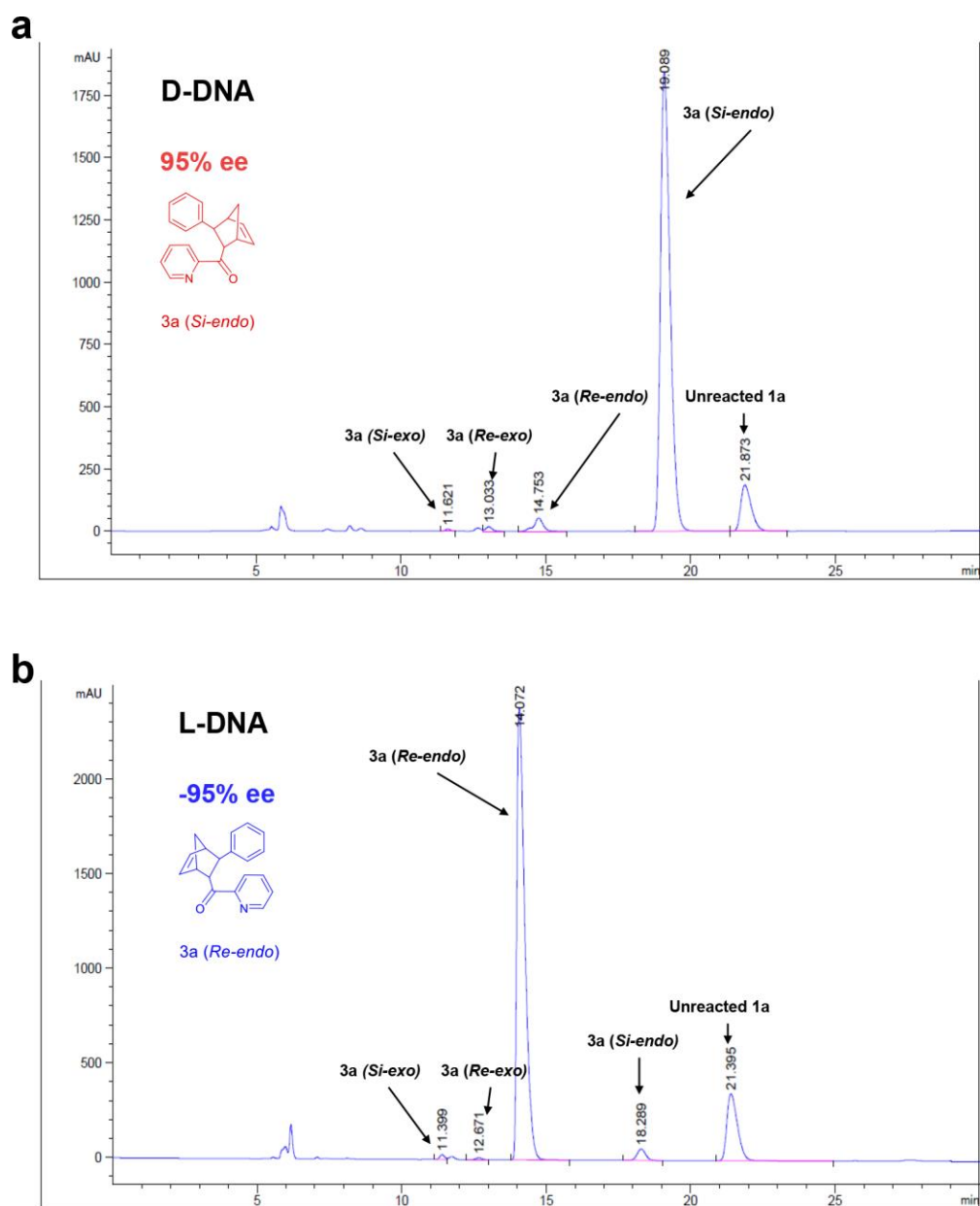


**Figure S27.** Melting curves of sequences (a) “8-4, 5”, (b) “8”, (c) HT21, and (d) st-DNA, all at 3  $\mu\text{M}$  in phosphate buffer. Measurements were taken at 268 nm at 0.2  $^{\circ}\text{C}/\text{min}$ . Representative curves are shown from three independent experiments.

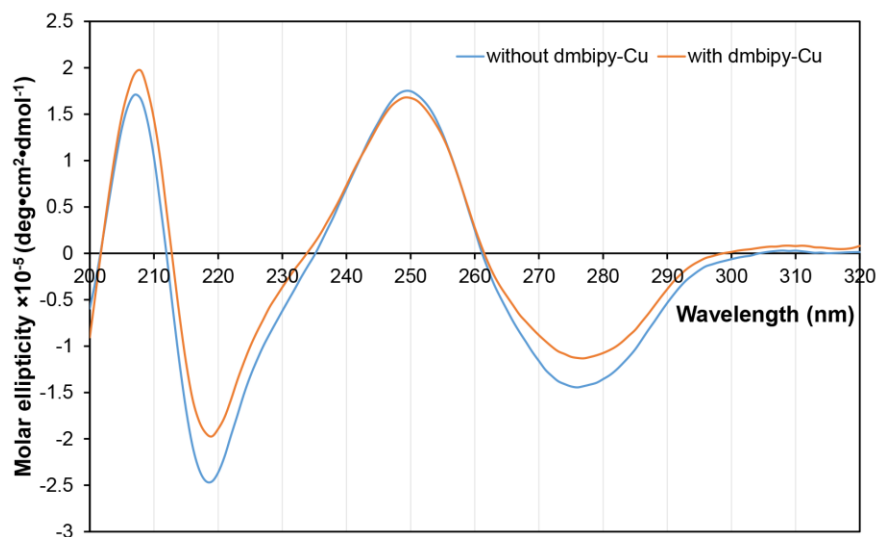


**Figure S28.** Binding constants of dmbipy-Cu to different sequences based on DNA base pair concentrations. Data are shown as mean  $\pm$  SD (n=3). Statistical difference was determined using one-way ANOVA with Tukey's honest significant difference post-hoc test; \* P < 0.05, for all other pairs with no brackets P > 0.05.

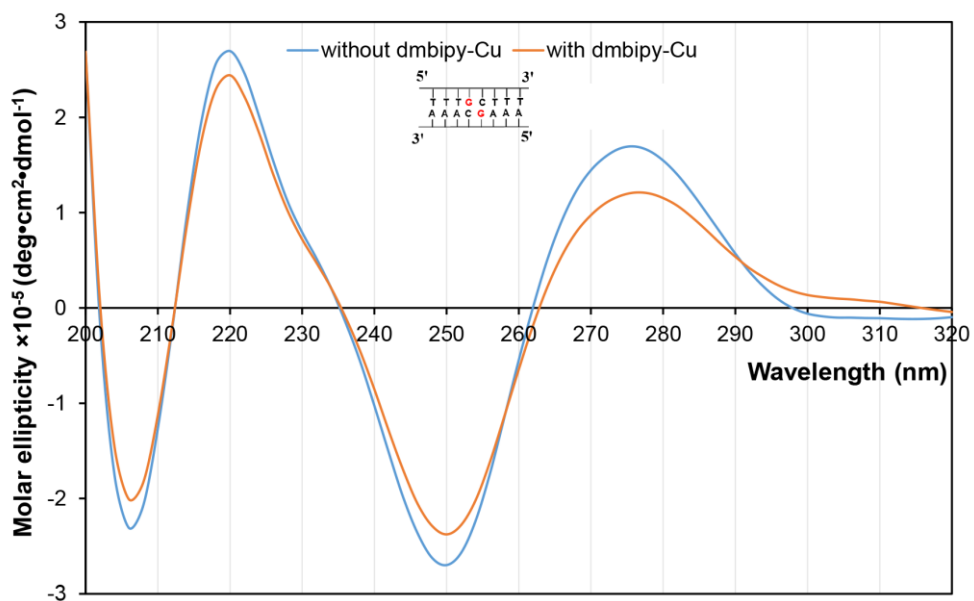




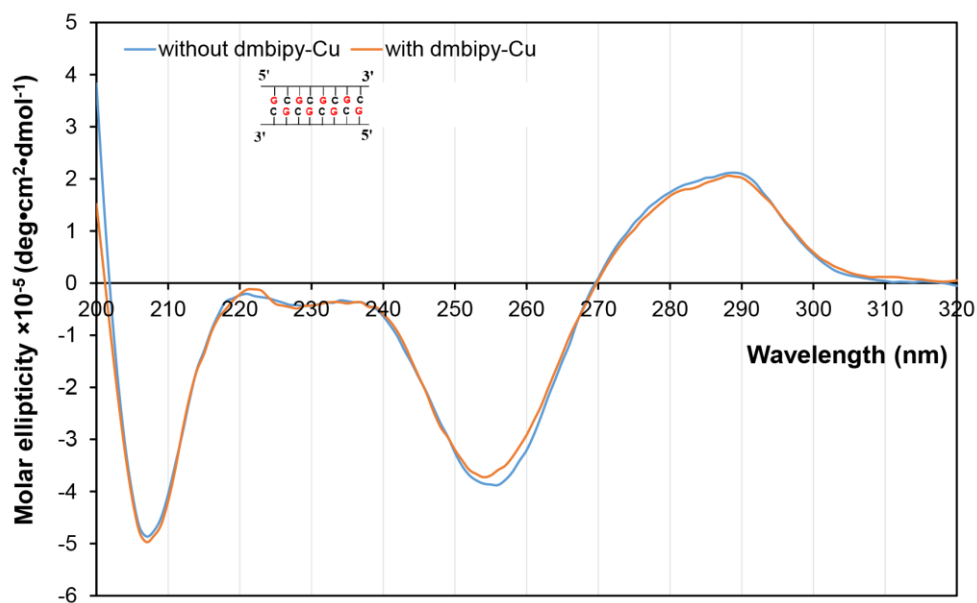
**Figure S29.** (a) HPLC trace for the Diels-Alder reaction mixture catalyzed by right-handed “8-4, 5” sequence with dmbipy-Cu (ee: 95%). (b) HPLC trace for the Diels-Alder reaction mixture catalyzed by left-handed “8-4, 5” sequence with dmbipy-Cu (ee: -95%). Same reaction and conditions as in Figure 1.



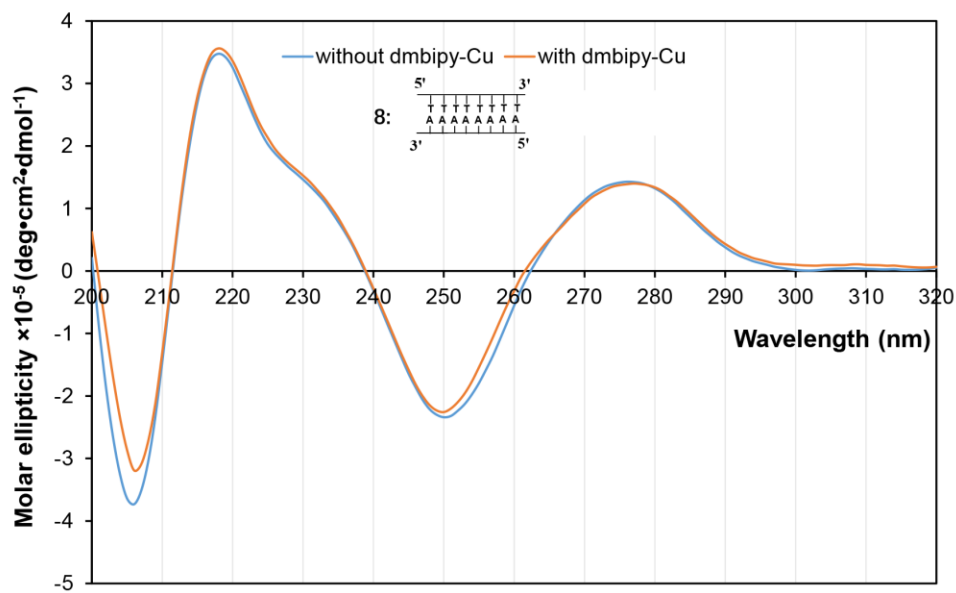
**Figure S30.** CD spectra of left-handed “8-4, 5” (50  $\mu$ M, in 20 mM MOPS buffer, pH 6.5) in the absence or presence of dmbipy-Cu (1 eq.).



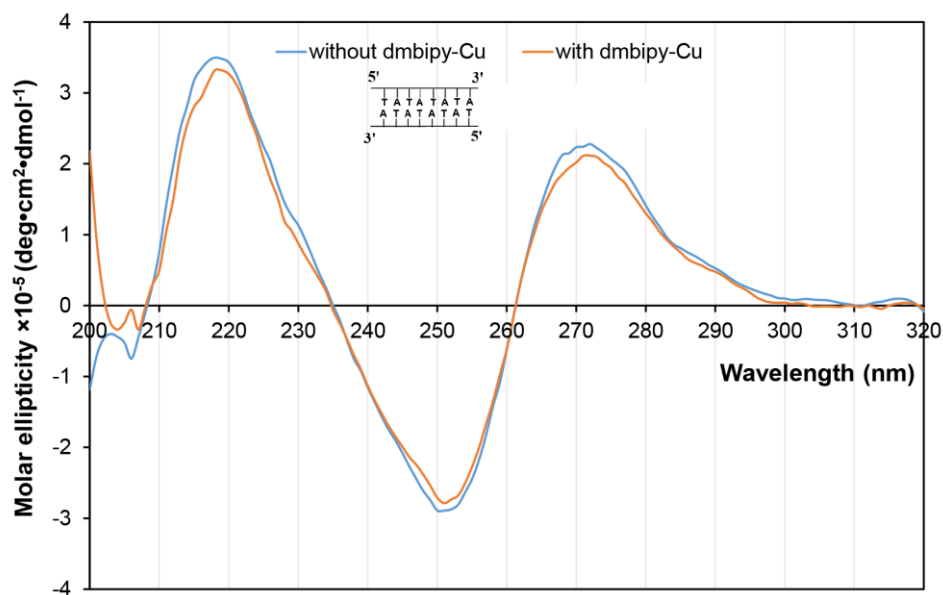
**Figure S31.** CD spectra of (TTTGCTTT) • (AAACGAAA) sequence (50  $\mu$ M, in 20 mM MOPS buffer, pH 6.5) in the absence or presence of dmbipy-Cu (1 eq.).



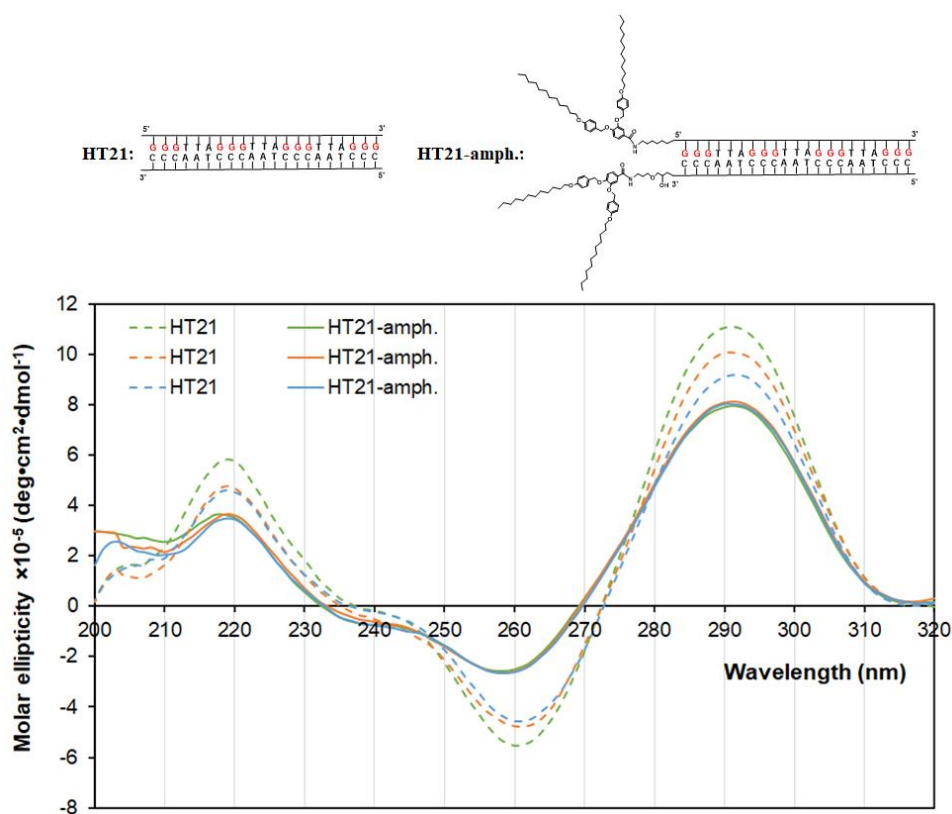
**Figure S32.** CD spectra of 8-base pair alternating G•C sequence (50  $\mu$ M, in 20 mM MOPS buffer, pH 6.5) in the absence or presence of dmbipy-Cu (1 eq.).



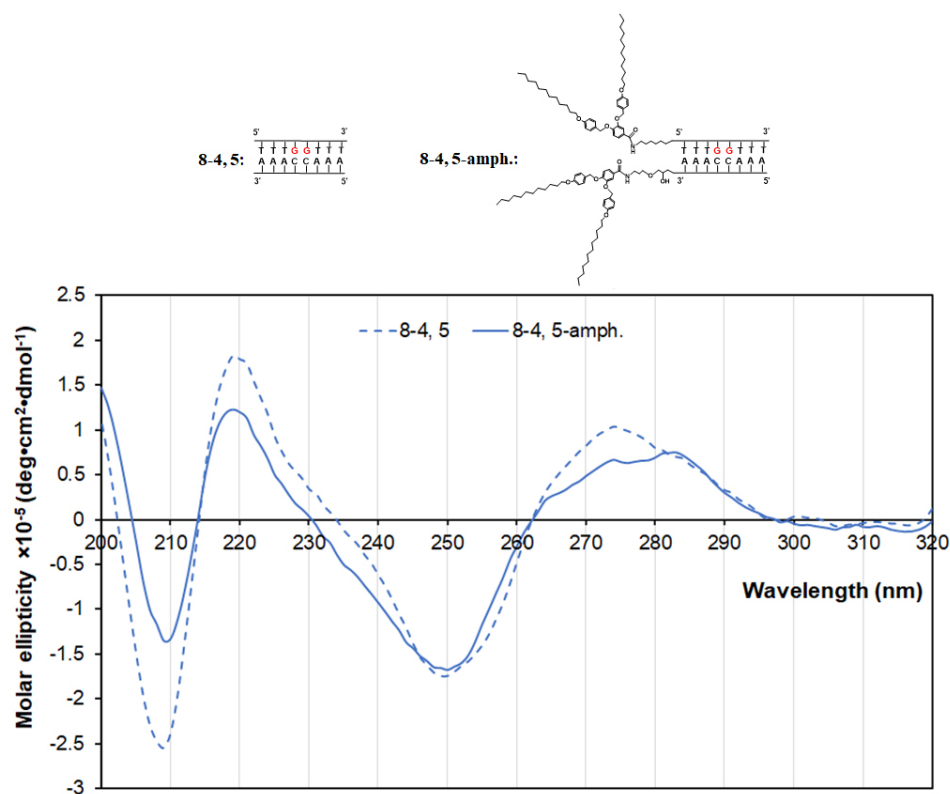
**Figure S33.** CD spectra of “8” sequence (50  $\mu$ M, in 20 mM MOPS buffer, pH 6.5) in the absence or presence of dmbipy-Cu (1 eq.).



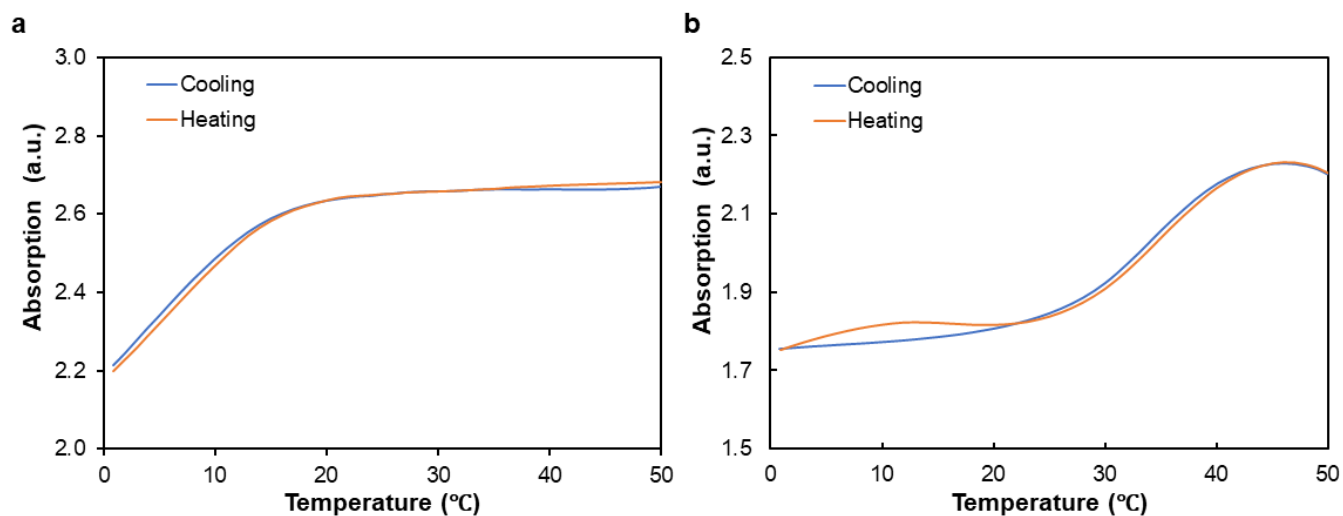
**Figure S34.** CD spectra of 8-base pair dsDNA based on alternative TA base pairs (50  $\mu$ M, in 20 mM MOPS buffer, pH 6.5) in the absence or presence of dmbipy-Cu (1 eq.).



**Figure S35.** CD spectra of HT21 and its amphiphile “HT21-amph.” in methanol-water mixture (v/v = 50/50), (15  $\mu$ M, in 20 mM MOPS buffer, pH 6.5) in the presence of dmbipy-Cu (1 eq.). Spectra are shown from three independent experiments.



**Figure S36.** CD spectra of “8-4, 5” and its amphiphile “8-4, 5-amph.” in methanol-water (v/v = 50/50) mixture (15  $\mu$ M, in 20 mM MOPS buffer, pH 6.5) in the presence of dmbipy-Cu (1 eq.).

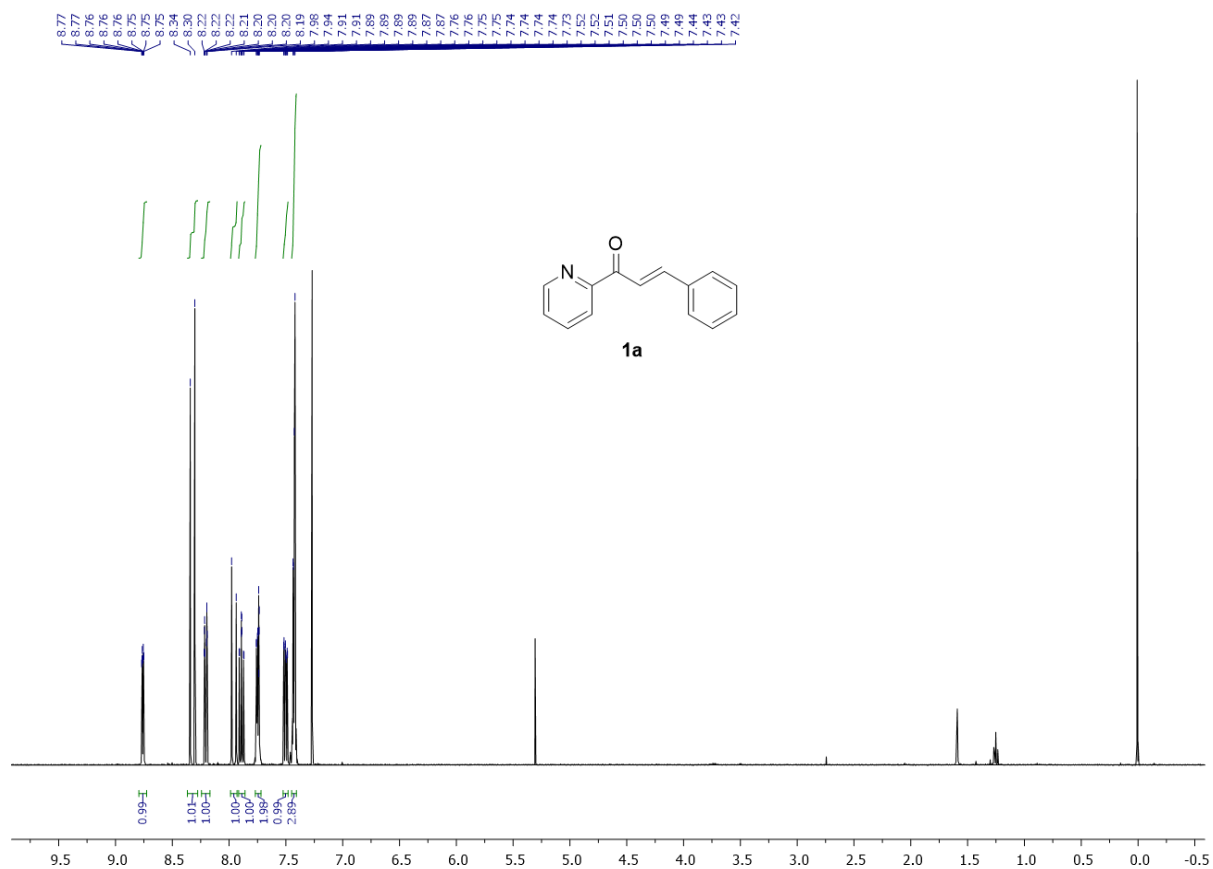


**Figure S37.** Melting curves of (a) “8-4, 5” and (b) its amphiphile “8-4, 5-amph.”, both at 15  $\mu$ M in a mixture of methanol and phosphate buffer (v/v = 50/50). Measurements were taken at 268 nm at 0.2  $^{\circ}$ C/min. Representative curves are shown from three independent experiments.

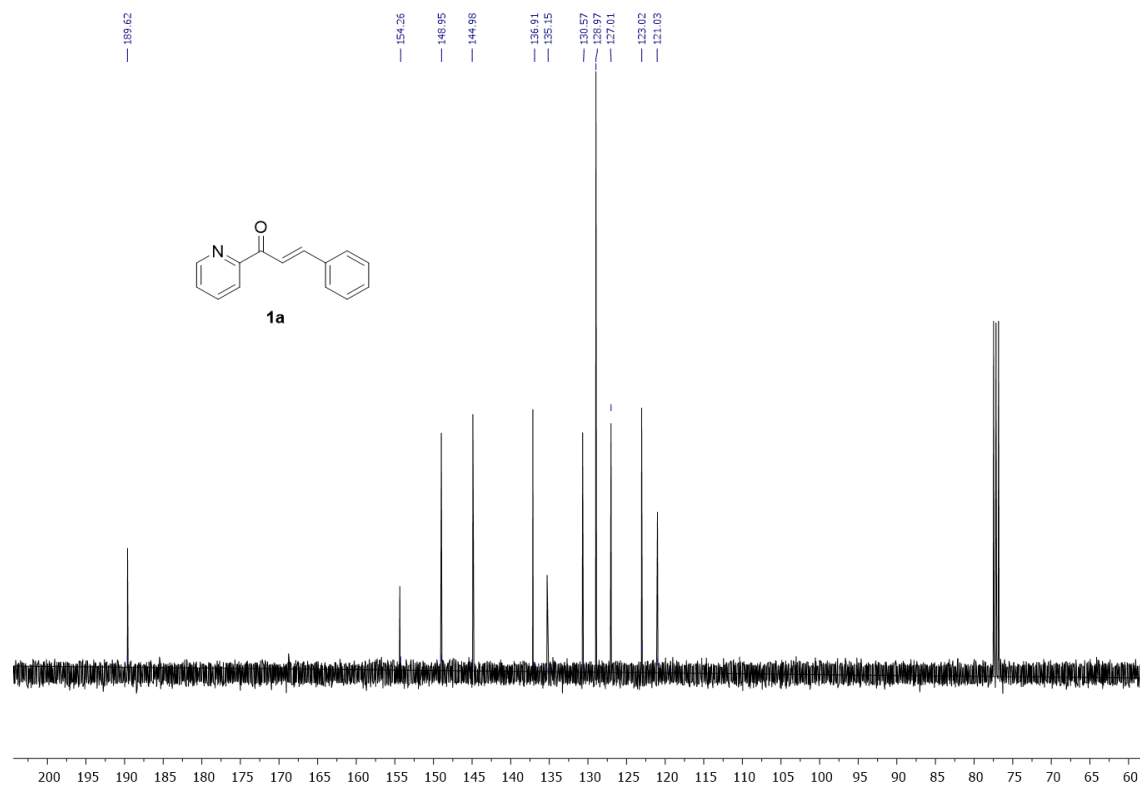
# <sup>1</sup>H-NMR Spectra and <sup>13</sup>C-NMR Spectra

(1) (E)-3-phenyl-1-(pyridin-2-yl)prop-2-en-1-one (**1a**)

**1a**: <sup>1</sup>H NMR (400 MHz, CDCl<sub>3</sub>) δ = 8.76 (ddd, *J*=4.8, 1.7, 0.9, 1H), 8.32 (d, *J*=16.1, 1H), 8.24 – 8.17 (m, 1H), 7.96 (d, *J*=16.1, 1H), 7.92 – 7.86 (m, 1H), 7.77 – 7.72 (m, 2H), 7.50 (ddd, *J*=7.6, 4.8, 1.3, 1H), 7.43 (dd, *J*=5.1, 1.8, 3H).

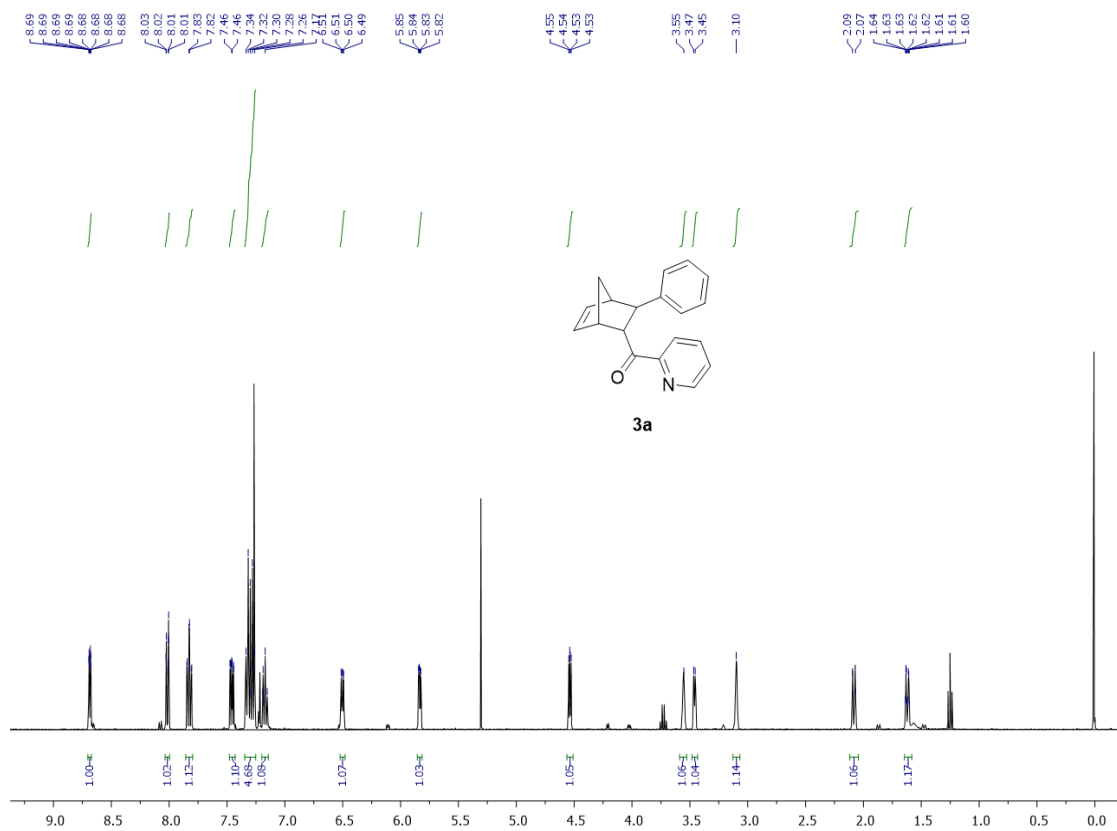


**1a**:  $^{13}\text{C}$  NMR (101 MHz,  $\text{CDCl}_3$ )  $\delta$  = 189.62, 154.26, 148.95, 144.98, 136.91, 135.15, 130.57, 128.97, 127.01, 123.02, 121.03.



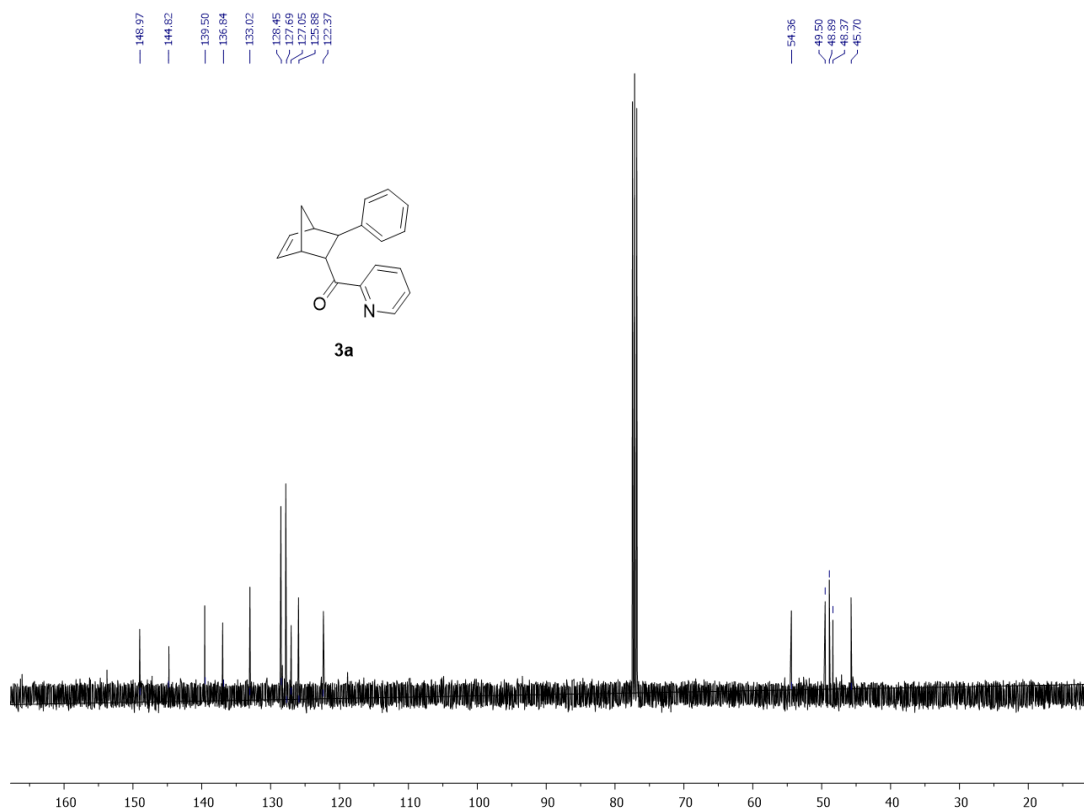
(2) 3-phenylbicyclo[2.2.1]hept-5-en-2-yl(pyridin-2-yl)methanone (**3a**)

**3a**:  $^1\text{H NMR}$  (400 MHz,  $\text{CDCl}_3$ )  $\delta$  = 8.69 (ddd,  $J=4.7, 1.7, 0.9$ , 1H), 8.01 (dt,  $J=7.9, 1.1$ , 1H), 7.83 (td,  $J=7.7, 1.7$ , 1H), 7.46 (ddd,  $J=7.6, 4.8, 1.3$ , 1H), 7.35 – 7.25 (m, 4H), 7.20 – 7.14 (m, 1H), 6.50 (dd,  $J=5.6, 3.2$ , 1H), 5.84 (dd,  $J=5.6, 2.8$ , 1H), 4.54 (dd,  $J=5.2, 3.4$ , 1H), 3.55 (s, 1H), 3.46 (d,  $J=5.2$ , 1H), 3.10 (s, 1H), 2.08 (d,  $J=10.4$ , 1H), 1.62 (ddd,  $J=8.6, 3.4, 1.7$ , 1H).

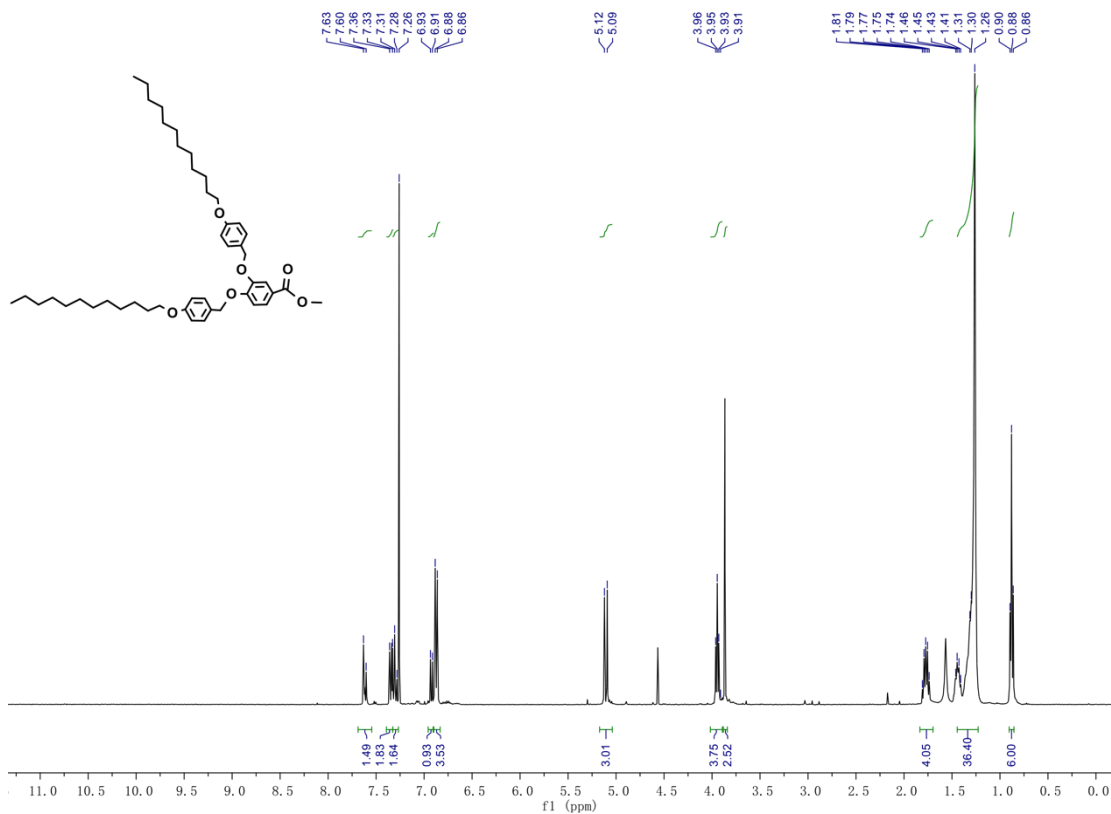




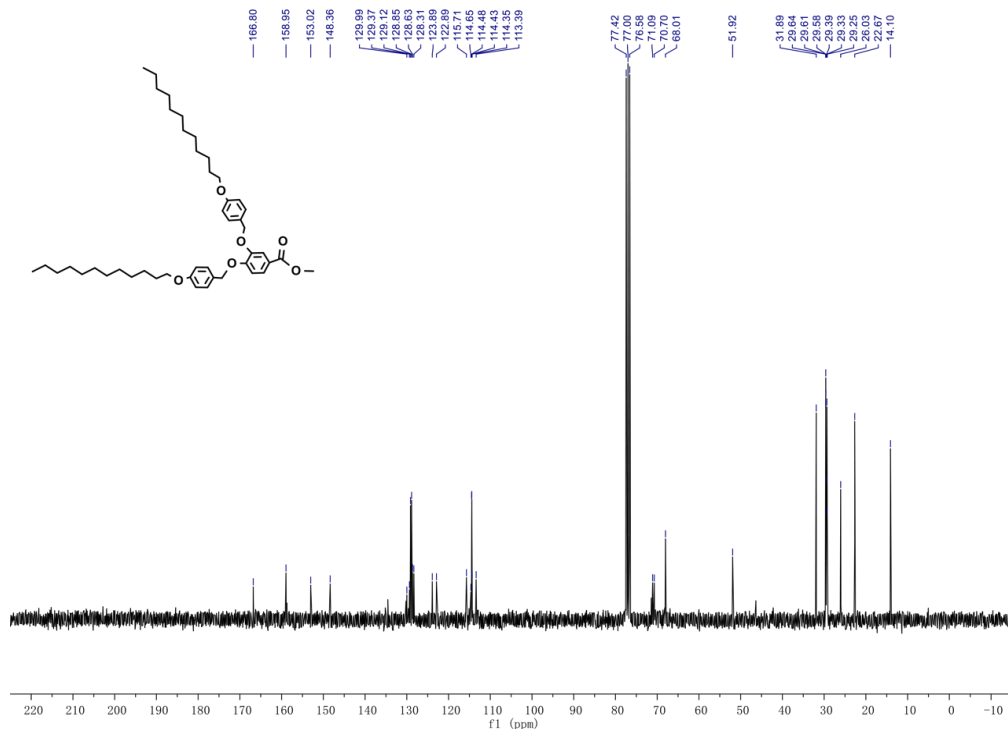
**3a:**  $^{13}\text{C}$  NMR (101 MHz,  $\text{CDCl}_3$ )  $\delta$  = 148.97, 144.82, 139.50, 136.84, 133.02, 128.45, 127.69, 127.05, 125.88, 122.37, 54.36, 49.50, 48.89, 48.37, 45.70.



Methyl 3,4-Bis[4-(n-dodecan-1-yloxy)benzyloxy]benzoate:  $^1\text{H NMR}$  (400 MHz,  $\text{CDCl}_3$ )  $\delta$  7.62 (d,  $J = 10.9$  Hz, 1H), 7.34 (d,  $J = 12.2$  Hz, 2H), 7.30 (d,  $J = 9.2$  Hz, 2H), 6.92 (d,  $J = 8.4$  Hz, 1H), 6.87 (d,  $J = 8.7$  Hz, 4H), 5.11 (d,  $J = 11.4$  Hz, 3H), 3.94 (q,  $J = 6.9$  Hz, 4H), 3.87 (s, 3H), 1.83 – 1.70 (m, 4H), 1.45 – 1.23 (m, 36H), 0.88 (t,  $J = 6.8$  Hz, 6H).



Methyl 3,4-Bis[4-(n-dodecan-1-yloxy)benzyloxy]benzoate:  $^{13}\text{C}$  NMR (75 MHz,  $\text{CDCl}_3$ )  $\delta$  166.80 (s), 158.95 (s), 153.02 (s), 148.36 (s), 129.99 (s), 129.25 (d,  $J = 18.5$  Hz), 128.74 (d,  $J = 16.9$  Hz), 128.31 (s), 123.89 (s), 122.89 (s), 115.71 (s), 115.19 – 113.89 (m), 113.39 (s), 77.42 (s), 77.00 (s), 76.58 (s), 71.09 (s), 70.70 (s), 68.01 (s), 51.92 (s), 31.89 (s), 29.64 (s), 29.61 (s), 29.59 (s), 29.33 (s), 29.25 (s), 26.03 (s), 22.67 (s), 14.10 (s).

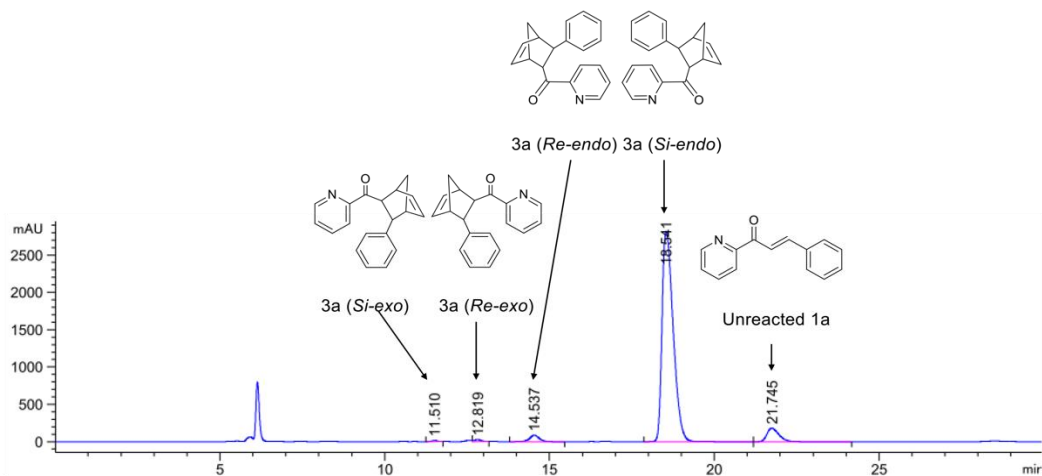


## HPLC Chromatogram

HPLC condition: Daicel chiralcel-ODH, hexane/i-PrOH 98:2, 0.5 mL/min, 212 nm.

Product **3a** from the Diels-Alder reaction catalyzed by dmbipy-Cu in the presence of "21-10, 11" sequence (ee: 95%).

Retention times: 11.5 (*Si-exo*), 12.8 mins (*Re-exo*); 14.5 (*Re-endo*), 18.5 mins (*Si-endo*).



Signal 1: DAD1 A, Sig=212,4 Ref=360,100

Peak #	RetTime [min]	Type	Width [min]	Area [mAU*s]	Height [mAU]	Area %
1	11.510	BB	0.1842	164.59950	14.00115	0.2264
2	12.819	VB	0.2183	396.77563	27.49980	0.5458
3	14.537	BB	0.2967	1765.10876	88.48657	2.4281
4	18.541	BB	0.3609	6.58296e4	2814.56226	90.5563
5	21.745	BB	0.3883	4538.60059	181.15187	6.2434

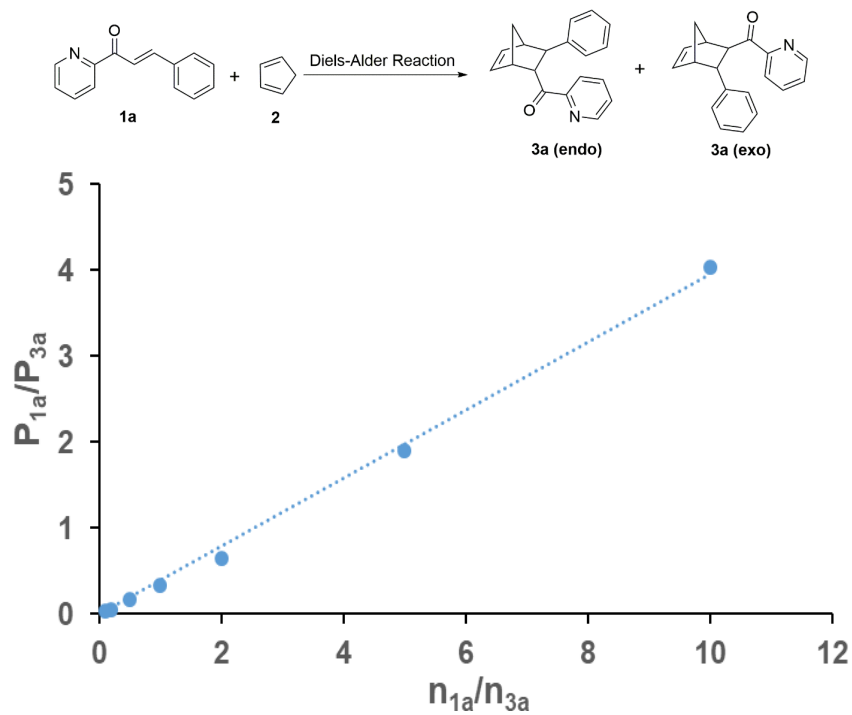
## Calculation of Conversion of (1a)

Conversion of **1a** was calculated based on the equation below:

$$\text{Conversion of } \mathbf{1a} (\%) = \mathbf{n_{3a}} / (\mathbf{n_{1a}} + \mathbf{n_{3a}}) = \mathbf{P_{3a}} / (\mathbf{P_{3a}} + \mathbf{P_{1a}} / \mathbf{k_1})$$

**P<sub>3a</sub>**: HPLC peak areas of **3a**

**P<sub>1a</sub>**: HPLC peak areas of **1a**



Determination of correction factor  $k_1$ . The HPLC peak areas ratios ( $P_{1a}/P_{3a}$ ) were determined with the standard molar ratios ( $n_{1a}/n_{3a}$ ) of 0.1, 0.2, 0.5, 1, 2, 5, 10. The correction factor  $k_1$  determined to be 0.396 ( $R^2 = 0.997$ ).